2016

In-Shoe Plantar Pressure System To Investigate Ground Reaction Force Using Android Platform

Ahmed A. Mostfa
Virginia Commonwealth University

www.manaraa.com

In-Shoe Plantar Pressure System To Investigate Ground Reaction Force

Using Android Platform

A Thesis submitted in partial fulfillment of the requirements for the
Degree of Master of Science at Virginia Commonwealth University

By

Ahmed A. Mostfa

Master of Science
School of Engineering
Electrical and Computer Engineering
May 2016

Director: Dr. Weijun Xiao
Assistant professor, Department of Electrical and Computer Engineering

Virginia Commonwealth University
Richmond Virginia
May 2016

Acknowledgment

Table of Contents

iii

iv

List of Figure

List of Tables

Abstract

Human footwear is not yet designed to optimally relieve pressure on the heel of the foot. Proper foot pressure assessment requires personal training and measurements by specialized machinery. This research aims to investigate and hypothesize about Preferred Transition Speed (PTS) and to classify the gait phase of explicit variances in walking patterns between different subjects. An in-shoe wearable pressure system using Android application was developed to investigate walking patterns and collect data on Activities of Daily Living (ADL). In-shoe circuitry used Flexi-Force A201 sensors placed at three major areas: heel contact, 1st metatarsal, and 5th metatarsal with a PIC16F688 microcontroller and Bluetooth module. This method provides a low-cost instantaneous solution to both wear and records plantar foot simultaneously. Data acquisition used internal local memory to store pressure logs for offline data analysis. Data processing used the perpendicular slope to determine peak pressure and time of index. Statistical analysis can utilize to discover foot deformity. The empirical results in one subject showed weak linearity between normal and fast walk and a significant difference in body weight acceptance between normal and slow walk. In addition, T-test hypothesis testing between two healthy subjects, with $\propto = 0.05$, illustrated a significant difference in their Initial Contact pressure and no difference between their peak-to-peak time interval. Preferred Transition Speed versus VGRF was measured in 19 subjects. The experiments demonstrated that vertical GRF averagely increased 18.46% when the speed changed from 50% to 75% of PTS with STD 4.78. While VGRF increased 21.24% when the speed changed from 75% to 100% of PTS with STD 7.81. Finally, logistic regression between 12 healthy subjects demonstrated a good classification with 82.6% accuracy between partial foot bearing and their normal walk.

Problem Statement

Muscles from mechanical movements may develop inflamed pain and plantar foot that is caused by foot overuse. Furthermore, the plantar foot could cause unbalanced walking that affects Vertical Ground Reaction Force during normal walking. The purpose of this study is to normalize the pressure percentage increases when the percentage speed increased between different subjects. In addition, the study is to assess and classify the pressure value between partial foot bearing and normal walking.

Chapter 1

Introduction

Plantar pressure analysis is one of the most important elements in managing the assessments of a client with diabetes and peripheral neuropathy. The indicated data from plantar foot pressure platform can be utilized in finding the impairments associated with various musculoskeletal and neurological disorders. The historical instrumentation used to analyze foot patterns belongs to Etienne-Jules Marey (1830-1904). Marey was one of the famous researchers in biomechanics and chronography. Marey implemented chambers in the shoes to show the timing of the steps during running. Marey also used the primitive accelerometer to measure the speed with a complete pneumatic recording system. He used a stereoscopic chronograph to better analyze both human body movements and animals. Vierordt (1881) followed Marey to be another investigator in foot pressure analysis. Vierordt used ink to spray from a nozzle attached to the shoe to detect foot pressure placements. However, the Weber brothers in Germany described the gait cycle in 1836 by making an accurate measurement of the timing of gait related with the pendulum swing of the leg. In the late 1970s, innovative researchers

noticed an essential development of gait measurements. The improvements of kinematic tools, based on electronics rather than photography measurements, reduced time and effort of analysis.

However, one of the fundamental approaches that identify the walking patterns is the Gait Cycle (GC). The functionality for each stride includes changing prejudices about the relationship between the foot and the body. This relationship generates the GC patterns, each in which related with different motions and performed by hip, knee, and ankle. As the body and foot transition, shock absorption demonstrates the progression of the body falling down and forward. During the GC, the only single sequence of functions that could appear generated by one limb. GC can identify the stance and swing. When the foot starts to contact with the ground, the stance is (60% of GC) introduced and it can be defined as the entire period when the foot is on the ground, and the swing (40% of GC) stands for the time when the foot is in the air for limb advancement [1].

1.1 GC Phases

The GC phases illustrated in the Figure below.
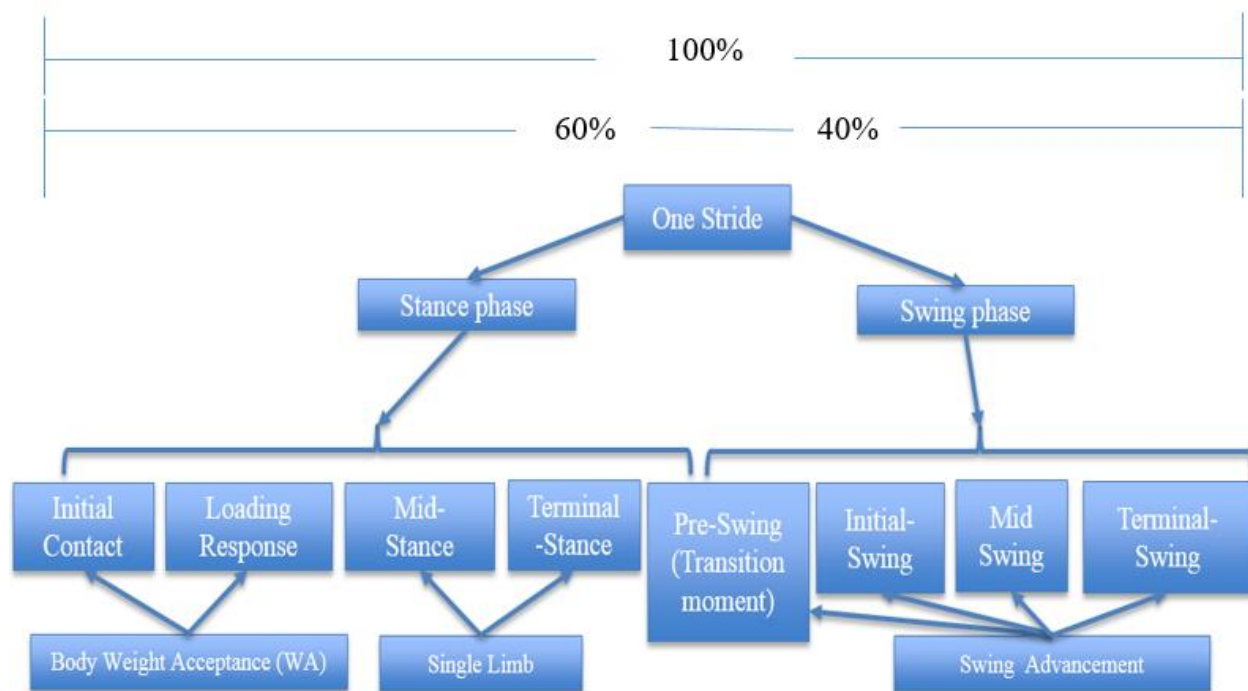
Figure 1 shows the gait cycle divisions

During walking patterns, the limb generates eight different phases called Gait Cycle (GC) phases. Within the phases, the function of different motions can occur for individual joints and identify the effects of disabilities. Each one of the eight phases has a specific role during the motion of steps. These phases are:

1-Initial Contact or the heel strike (IC 0% to 2% of the GC) is implicit of the impact transient, heel rocker, and heel first contact. At this moment, the body's muscles at the ankle, knee and hip work on absorbing the shock of the floor during progression. The essential impact of the

abrupt (foot-to-foot) can generate a vertical spike during the Ground Reaction Force (GRF). The transit impact could reach 50% to 125% of the body weight as illustrated in Figure 2.
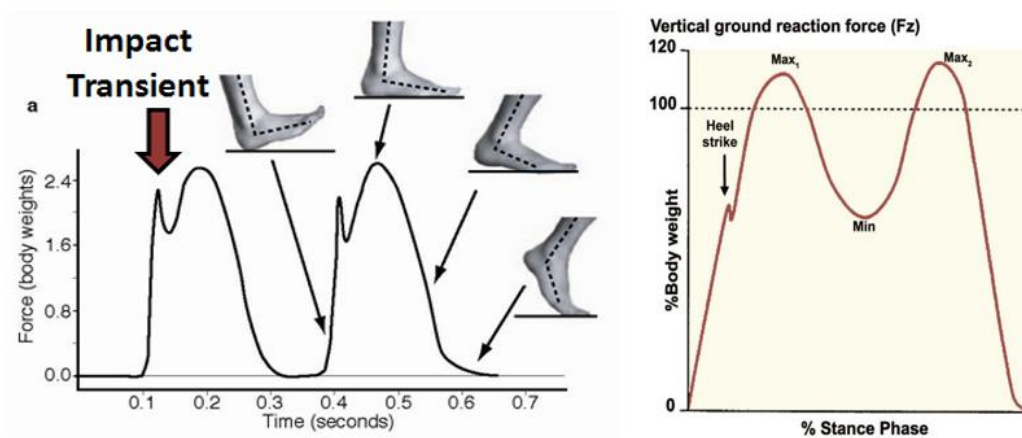
Figure 2 shows the heel strike at Initial contact during the GC [3].

2- Loading Response (2% to 12% of GC). The goal and the parameter can determine are the shock absorption, weight bearing, and progression.

1.2 Shock Absorption

Perry and Burnfield define the keyword weight acceptance (WA) as the weight moving from constant stability to the position of falling down [1]. The impact of weight acceptance can be reduced by shock absorbing reactions. The body parts that are affected by shock absorption are the ankle, heel, and knee. The pretibial muscles restrict the ankle and create a delayed contact between the foot and the ground (12% of the GC). This delay in the loading response, between the foot and the ground, is depicted in Figure 2, in which the graph represents the two peaks

and one valley of the GRF. The first peak represents the rapid transit impact (approx. 0.02 secs.) caused by the heel [1]. The second peak is caused by the forefoot making contact with the ground. Each peak is approximately 110% of the body weight while the valley estimates 80%. Another factor that encumbers shock absorption is the knee flexion, related to the tendinous attached to the tibia and fibula, that causes the leg to follow the foot.

However, the vertical forces from the peaks can change based upon the walking velocity patterns. Walking slower may reduce the vertical acceleration of the peaks while walking faster may generate a higher peak and lower valley. In the running process, the peaks can reach up to 2.5 times the body weight [4]. Furthermore, one can conclude that the peak load of the GRF can determine the loading rate from the limb, which can affect the gait velocity.

3- Mid Stance (12% to 31% of GC). It represents the first half of the limb mobile source.

4- Terminal Stance (31% to 50% of GC). It appears when the heel starts to rise up and leave the ground while the body leans forward to begin the progression of the body.

5- Pre-Swing (50% to 62% of GC). It begins when the initial contact (IC) of the second limb, through the end of toe-off.

6- Initial Swing (62% to 75%). In here, the foot would lift off and the second foot is at mid-stance phase.

7- Mid Swing (75% to 87% of GC). Where the limbs swing forward to the hip flexion and the foot is off the ground.
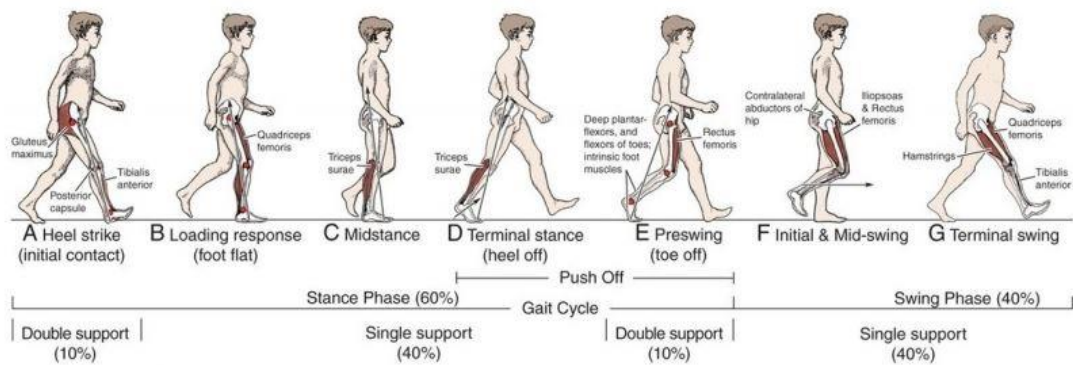
Figure.3 The process of one stride of the eight phases Gait Cycle [2].

8- Terminal Swing (87% to 100%). This is the final phase where the foot is preparing to make its initial contact with the ground using the vertical tibia. The Figure 3 shows the 8 different phases enclosed.

1.3 Foot Measurements Technology

It is important to measure the foot parameters in order to assess empirical results. Parameters can be categorized into three types: spatial, temporal, and combined. The spatial parameters are the stride length, step length, and base support width. The temporal parameters are the swing time, stance time, single support time, double support time, and gait cycle time. The combined parameters are the average walking velocity and cadence.

One of the physical assessment methods is to ask a subject to walk and find the time (t), and distance (d) elapsed. Where the velocity is:

$$v = d/t$$

The cadence can be determined by the number of steps divided by the time measurement from beginning of the step to the last step,

$$c = n/T(n)$$

While the average step length (l) can be measured by the distance (d) divided by the number of steps (n).

$$l = d/n$$

Since the complete stride includes two steps, then the average gait cycle time (Tg) is

$$Tg = 2t/n$$

The tools of any system that are used to measure the plantar foot consists of a device that might be a platform or insole, and a computer or mobile device to monitor and analyze the data stream. One of the methods used to determine the spatial gait parameters is the walkway marking method [5]. This clinical method would explicitly record the imprint parts of the foot, then the subject would walk over a thin metal foil. The markers on the walkway can make a subject changed his/her normal walking over unusual papers. Therefore, data processing would be time-consuming due to the manual measurements. For temporal variables (swing time, stance time, etc.), a stride analyzer is one of the examples that use pressure sensitive switches attached to subject's foot. Stride analyzer considers a better way to determine time information than the walkway marketing, but it is not suitable for the subjects who need an orthotic device within his/her shoe. It also still needs a complete set of insoles for each subject.

Meanwhile, a lot of commercial systems for measuring plantar pressure appeared (Emed sensor platform, Pedar insole system, F-scan system, and Musgrave footprint system) to collect the

data in both spatial and temporal gait. Data acquisition from plantar pressure can be used for evaluation patients with a variety of impairment that is related to neurological disorders.

We aim in this study to statistically classify the walking patterns of one subject, and also between two subjects. We questioned at what percentage the average peak pressure would increase if the speed changes from 50 to 75% of preferred transition speed (PTS). The logistic regression used peak pressures as one parameter between eight healthy subjects, to classify between their partial foot bearing and their normal walk.

This study is categorized into the following chapters:

Chapter 2 Literature Review will show the related works and research wherein different approaches (sensors, circuits, and design) to evaluate plantar foot were used.

Chapter 3. Plantar Pressure Assessment and System Circuit will discuss the sensors calibrations, statistical approach to valid force sensors, circuit design, and PCB.

Chapter 4 Android IDE Platform Implementation and data analysis. In this chapter, we will demonstrate the process of the app developments, sensors placement, trials, and basic statistical approach for results obtained and PTS hypothesis.

Chapter 2 Literature Review

Chapter 2 will illustrate research in orthopedic and therapeutic insole developments. A literature review is considered a helpful tool to highlight the causes and prevention of overuse injuries. Overuse injuries are commonly seen in eight regions of the foot (rear foot RF, medial midfoot MMF, lateral midfoot LM, middle forefoot MF, middle forefoot MDF, lateral forefoot LFF, hallux H, lesser toes LT), as shown the Figure 4. Robin M. Queen et al [6] discussed forefoot loading during three athletic tasks (Crossover Cut, Side Cut, and Forward Acceleration) in 36 subjects (17 women and 19 men with average weight 71 kg) using appropriate test size shoes from Pedar-X. Queen's outcomes highlighted the movements that may cause injuries in a specific region of the foot. Plantar pressure variables obtained from this study were peak pressure, force-time integral and contact area for each subject and for each individual foot. In addition to the results of the study highlighted, the consideration of force-time integral is essential to measure how long the area is under stress.
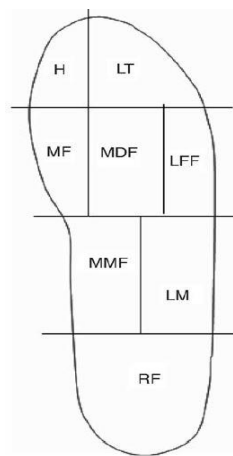
Figure 4 shows the classification of the foot in eight different regions [6].

Lin Shu et al. discussed an in-shoe plantar pressure data acquisition, with a wireless Bluetooth module that transmits the data [7]. The sensor used in this study was textile pressure fabricated by adhering fabric with conductive yarns. The sensor measurement ranges between 8Pa to 800KPa. Six sensors were used on a single point region at the heel and Metatarsal with a voltage divider circuit, and10-bit A/D PIC18F452 microcontroller as
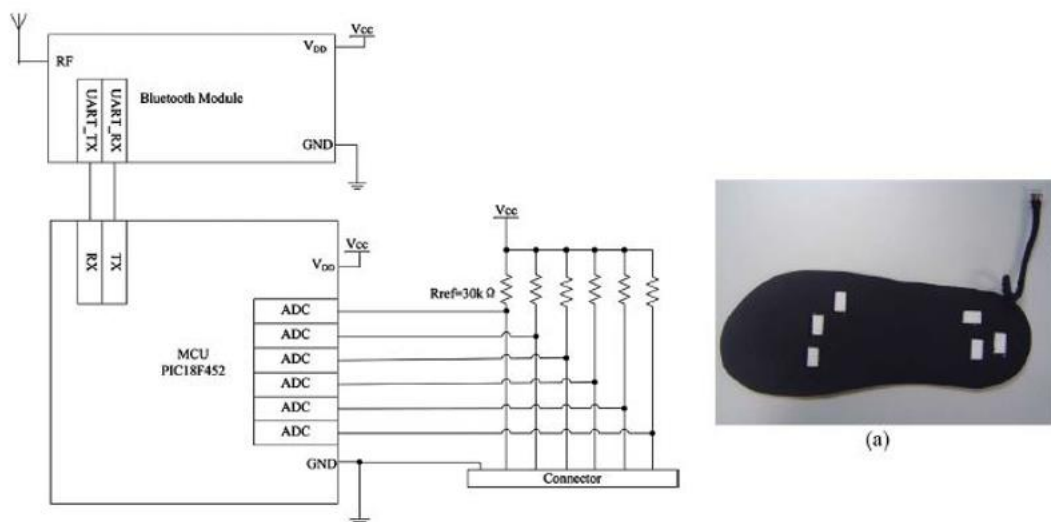
Figure 5 shows the voltage divider with six sensors attached [7]

shown in Figure 5. The system used a desktop, laptop, and smartphone to measure the mean pressure, peak pressure, center of pressure, and speed of the center of pressure. The study measured the standing and dynamic walking on the right foot. Lin Shu et al. results for the maximum mean pressure of the right foot was 200KPa, and the largest peak pressure was about 350KPa. The system measured the foot balancing during walking and running of activity daily

life (ADL), the circuit used a voltage divider that is very nonlinear for measuring the pressure

based upon Flexi-Force sensor Tekscan datasheet.
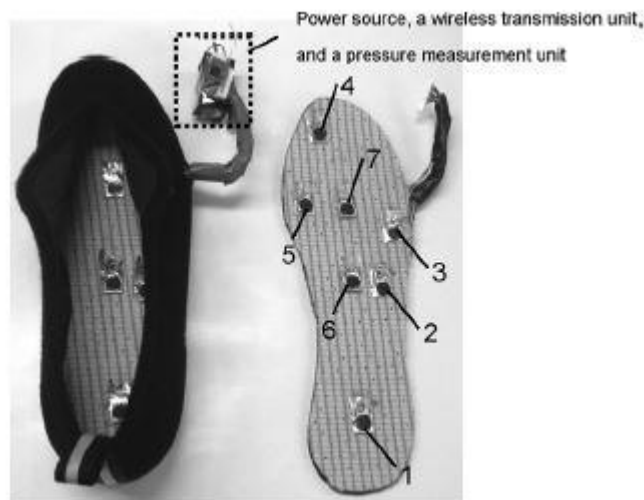
Figure 6 shows the PSCR sensors distribution at seven areas [8].

Saito et al. [8] developed seven pressures-sensitive conductive rubber sensor (PSCR) that can

stimuli between the ranges 25 to 250KPa. The sensors calibrated and measured to have the

same load during the activity. The sensors were individually conducted from each sensor to

have 10-bit analog-to-digital converter with sampling rate 20Hz. PSCR were placed according

to gait kinetics and pathological foot anatomy (Heel #1, lateral midfoot #2, lateral forefoot #3,

great toe #4, head of the first metatarsal #5, center of midfoot #6 and center forefoot #7). The

device was validated with F-scan (Tekscan, Inc., Boston, USA), and results for curves from

both devices illustrated that the peak pressure value at sensor #4 was 75.4KPa with Saito system

device. While in F-scan, the system showed 78.3KPa at #4. The differences in peak pressure

were between 2.9 to 29.3KPa (44%) at H, LM, LFF, GT, and CFF. Saito et al. study recruited

22 women who were 89 years old and had a body weight 40 to 45 kg. The results based on

monitoring the chart graph outcome from the motion showed pressure at #1 (heel) was increased when the first initial contacts happened. Pressure then moved towards midfoot and the toe. The in-shoe system was able to fit with different foot sizes and with energy efficiency for more than 20h, but the disadvantage appears in the sensors. Sensors have to calibrate each time the gait measurements begins
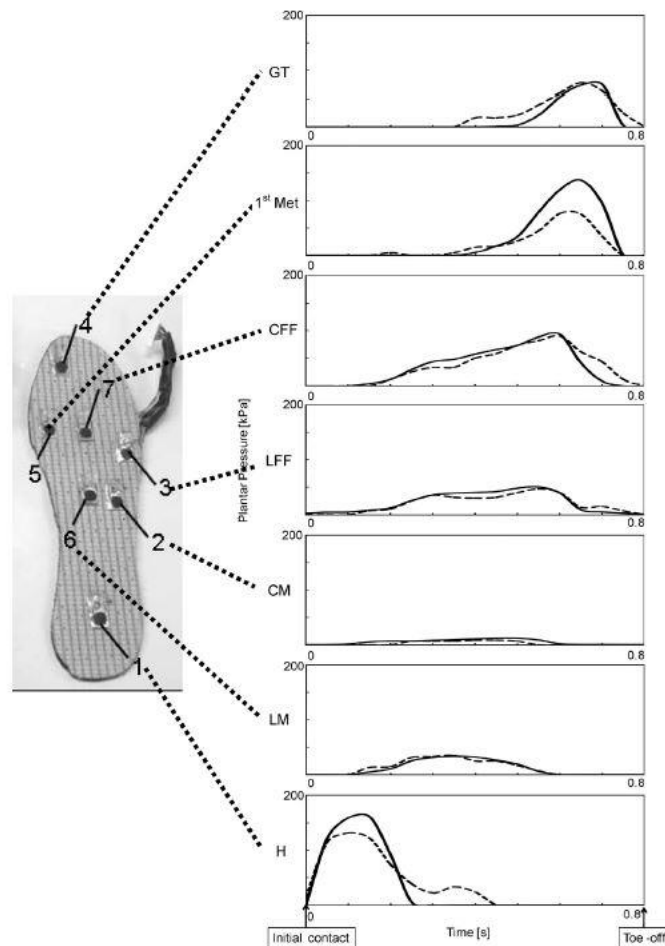
Figure 7 show the outcome results of each sensor distributed inside the in-shoe [8]

because degradation of the PSCR may occur over time. Furthermore, Saito did not mention which variables are able to measure figures beside peak pressure. Meng Chen et al. [9] shows the gait detection for abnormal walking patterns (Toe in, out, over supination, heel walking, and normal walking). Meng Chen used Principal Component Analysis (PCA) to reduce the dimensionality of the transformed data and Support Vector Machine (SVM) for multi-classification Figure 8.
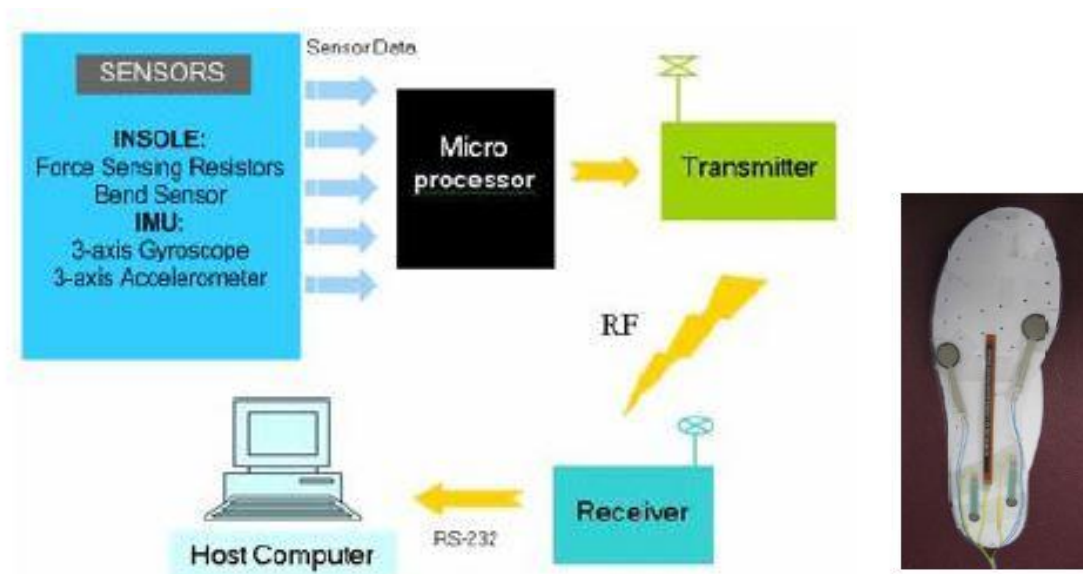
Figure 8 shows Meng Chen system outline architecture [9]

The figure shows insole, inertial measurement unit IMU; microprocessors based data and wireless communication system [9].

Four force sensors (FSR) and bend sensor, as shown the Figure above, used with a voltage divider to obtain the relationship between the force and voltage. The system used IMU with

three signal axis gyroscope and three-axis accelerometer to find the angular rates and accelerations. The data acquisition methods can be done by storing the data into local memory and then upload/download the data to a PC for further analysis, or it can be done while the data is transmitting at a real time. The system processed data in this study on a run time, but there were restrictions and transmitting errors. However, the process of SVM Figure 9 multi-classifier works as following:

- The data collected from normal walking for toe in, toe off, over supination and heel walking.
- Fast Fourier Transform (FFT) was used to analyze the data in frequency domain.
- Apply Principal Component Analysis (PCA) was used for modeling human gait patterns.
- Support Vector Machine was used to set training data for some input space X via the nonlinear function (One-against-one and one against-Rest).
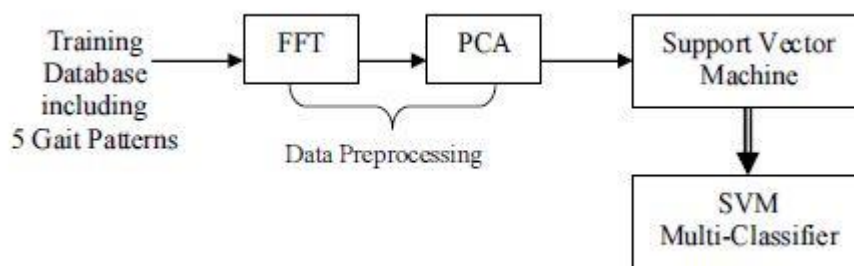
Figure 9 shows the SVM training data process [9].

The results obtained from subjects were used to demonstrate data classification for both feet (left and right). The training data segmented into $3010 \, X \, 22 \, matrix,$ then applied FFT, PCA to reduce segmented data. The transfer of selected data was utilized to determine the best SVM training and best success rate. The comparison results for one subject is shown in Figure 10. The system used insole sensors and IMU sensors input in order to have the best average rates and better detection results.

Gait Pattern	Success Rate	
	Insole	IMU
Toe in (1000 samples)	82.3%	84.7%
Toe out (1000 samples)	94.5%	90.9%
Oversupination (1000 samples)	96.9%	74.2%
Heel Walking (1000 samples)	85.4%	79.5%
Normal Pattern (1000 samples)	85.1%	79.4%
Total (5000 samples)	88.84%	81.74%
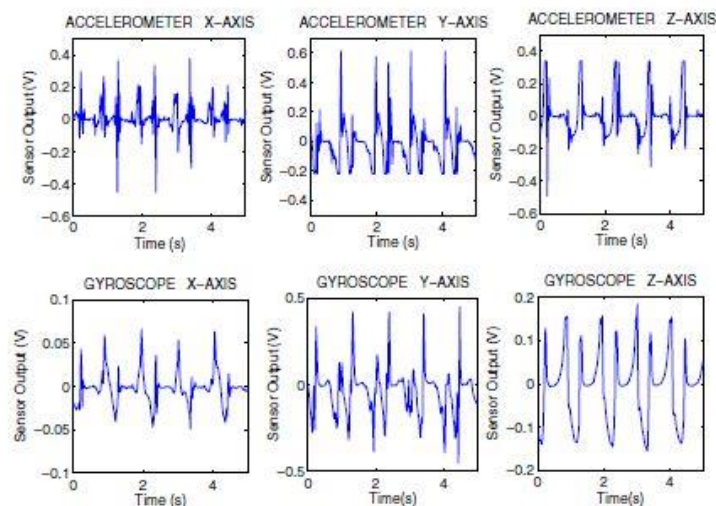
Figure 10 shows the parameters of angular acceleration and the comparison of the gait patterns for insole and IMU [9].
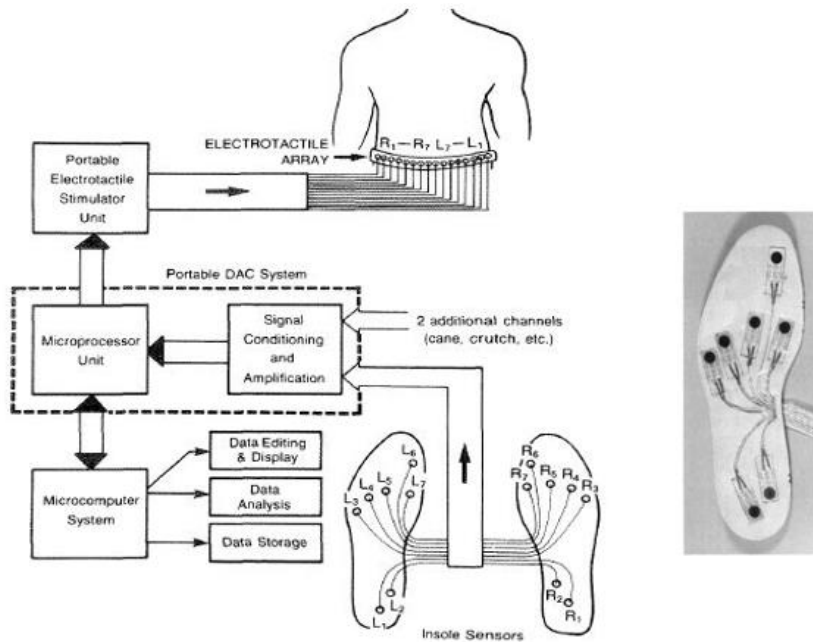
Figure 11 shows the insole portable system with the seven conductive polymers distributed over the heel, metatarsal, and great toe [10].

Wertsch et al. [10] developed an insole plantar pressure (portable to record for 2h) that has 7 sensors in each foot, which can be seen in Figure 11. The sensors used in this study were a conductive polymer with 0.25mm thickness. Wertsch set the characteristic roles for the sensor used in motion measurements so that it included the response time, low power consuming, low hysteresis and highly desirable sensitivity for temperature and humidity, and the ability to stimuli between the ranges 0 to 1.2MPa. Wertsch had demonstrated the footprint techniques to properly place the sensors like APEX foot imprinter, microcapsule socks, and Fuji Pres-sensor Mat. Although this study used a sensor that is inexpensive and has a longtime withstand, the disadvantage was the linearity moderate hysteresis [10]. It used a portable electrical stimulator in which it has a back to carry during ambulation. The study considered an old technology to

determine the GC variables. He did not reveal the potential outcome and experiments from the system. The conclusion states the system used in studying sensate and insensate plantar pressures, shuffling gait and loading patterns[10].

Klimiec et al. [11] developed an Electronic measurement system of the foot. He used polarized polyvinylidene fluoride (PVDF) foil as a seven sensors for measurements with total thickness 4mm which is shown in Figure 12. The construction of the sensor allows for suitable bending, twisting and resizing for sports purposes. The data acquisition circuit used seven amplifiers, ADC converter with high pass filter estimated with a cut-off frequency of 0.08Hz. The data then transferred using a Bluetooth module (Figure 13) to a desktop. Microsoft Excel was used to interface and classify the distribution of pressure across the foot. He did not go through the analysis of the Gait Cycle. Such as, the number of steps taken from subjects, time to peak, peak to peak, or weight bearing. Instead, Klimiec sufficiently discussed the sensor implementation, characteristics, and data transfer unit.
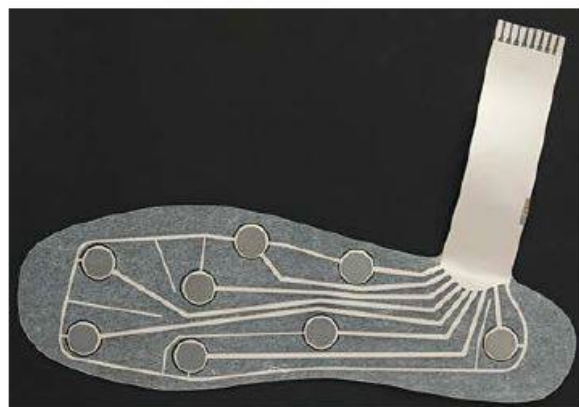
Figure 12 shows the PVDF sensors distribution used in Klimiec study [11].
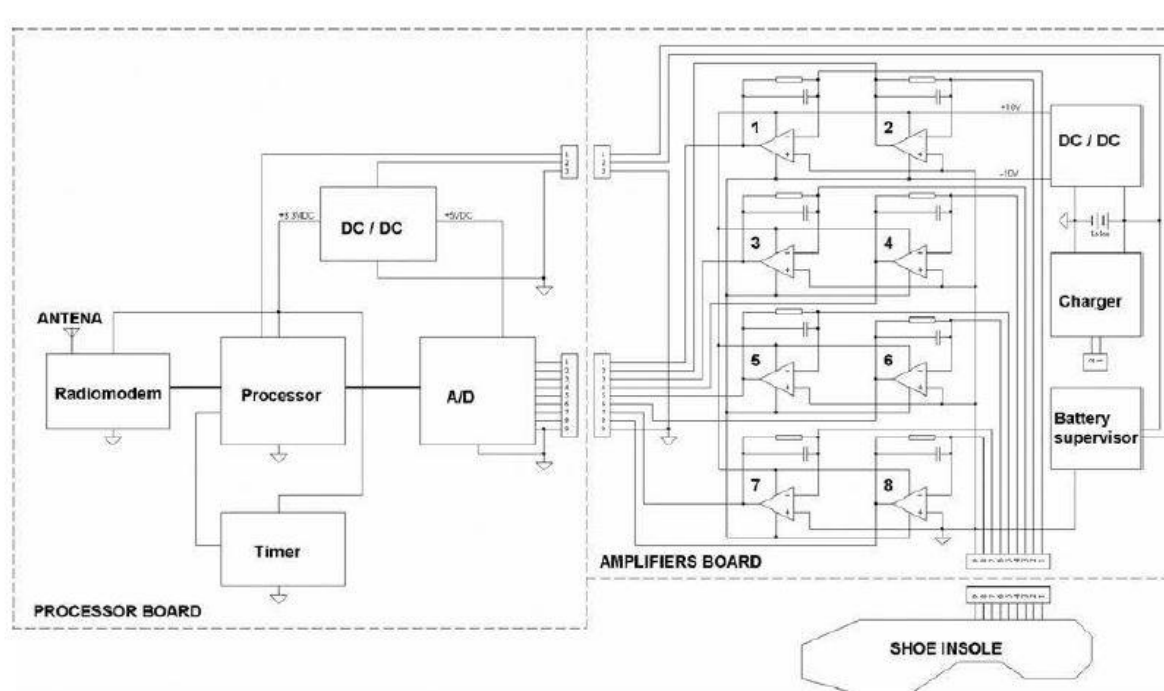
Figure 13 shows the system circuit architecture [11].

New techniques to measure foot gait used inertial sensors. Previous studies noticed that inertial sensor gait decreased in accuracy as gait velocity increased. Nevertheless, another study showed a variety of inertial sensor placed on the body and reported the ground contact and loss contact (heel and toe off). In addition, differences in walking and running were reported as an indication of peak pressure events. Little Chris and Bruce Lee James - in "the evaluation of inertial sensor technology in the discrimination of human gait". He determined whether temporal gait parameters can be identified between a normal fast walking, and running by using the inertial sensor to extract relative timing of heel contact within Vertical Acceleration Step Cycle (VASC).

Chapter 3 Plantar Pressure Assessment and System Circuit

3.1 Plantar Pressure Assessment

In the earlier study, we have introduced the fundamental keywords of the pathological foot analysis. However, specifications should consider when a one selects system measurements for the plantar foot might classify into resolution, sampling frequency, reliability, and calibration.

3.1.1 Resolution

It explains the size and number of sensors used to measure the motion - the higher resolution achieves when a higher number of sensors used. The size of the sensors could change the readings. When a force introduced to a large sensitive area, it will not offer the same pressure reading from the small sensing area [12]. The standard of $1 \ N/cm^2$ equals 10 KPa. If a 10N applies to a 1-cm^2, then the resulting pressure is 100 KPa. However, if the same force applied to a 4-cm^2 sensing area, the resulting pressure is 250KPa: the resolution can appear critically in a child's foot [12].

3.1.2 Sampling Frequency

The sampling frequency can play the roles in managing the temporal resolution of the system. It is defined as the number of samples generated from each sensor or from all sensors (depends on the method used to find the GC pattern) per second and recorded in hertz (Hz). The recommended sampling frequency for pressure is 50 to 100 Hz for walking and 200 Hz in running. We will highlight the sampling frequency of our PIC16F688 Microcontroller in the later chapters.

3.1.3 Reliability

The reliability of the measurements is also considered as one of the factors affected on the accurate measurements. The reliability could be found in average walking to ensure the repeatability of motion. It can also be found in sensor manufacturing and finding the sensor error during the running time.

3.1.4 Calibration

The keyword, calibration, is used to validate sensors performance. Part 3.3.3 will explain more details about calibration in this study.

The system was conditioned and calibrated in Dr. Xuejun Wen's lab, Department of Chemical and Life Science Engineering VCU. The A201 FlexiForce sensors were used in this study, while the system force used for calibration, shown in Figure 14, was the EZ Graph [13]. The calibration is useful to mitigate the effects of drift and hysteresis.

Figure 14 shows the EZ Graph 10N. This force system was used to calibrate the A201 Flexi-Force sensor.

3.2 Sensors

The most important part that regulates the pathological assessments and manages the motion behaviors can be estimated by many factors. Such factors would be the quality performance of sensors (manufacturers and weather changes), the flexibility of movement (wearable in-shoe or in a platform sensors), thickness, responses time, and linearity.

3.2.1 Sensor Placement

The method used to reduce the pain or injuries in the foot was by reducing the offending pressure. This can be done by decreasing the force or increasing the area of force as discussed. An in-shoe pressure assessment explains the mechanical stresses of the foot. To do this, the in-shoe sensor has to be thin in order to fit inside the shoe. Another quality of shoe sensor arrays must be able to be cut to fit the shoe. Figure 15 shows the matrix sensors that give enough mapping for the motion.

1A   **1B**
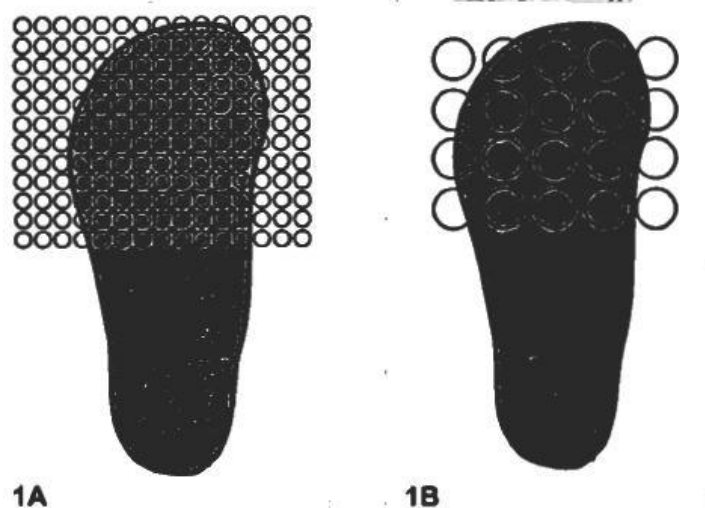
Figure 15 shows the matrix sensing area distributed along with the shoe [14].

The structure of the foot divided into 15 areas, as a heel (1-3), midfoot (area 4-5), metatarsal (6-10), and toe (area 11-15). The area analyzed can demonstrate the body balance to find the function of the limbs as shown in figure 16.

Placing the sensors in-shoe can vary from system to system based on the measuring parameters, like weight bearing, the center of pressure (COP), peak-to-peak time phase time, etc.
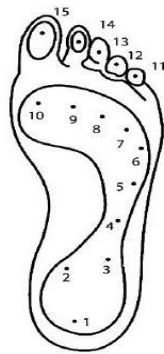
Figure. 16 shows the foot sensing area distribution according to Lin Shu et al [7].

3.2.2 Sensor Category

3.2.2.1 Platform Systems

Figure.17 shows the Emed and Pedar Novel plantar pressure system [15].

The instrumentation of platform contributed in the research of gait analysis and became the standard tools in almost every laboratories. The first platform designed by Amar in 1924 and enhanced by Elftman in 1938 [15]. Platform sensors usually arranged in arrays to pursue the sensing area of the entire foot. It could use for analysis the dynamic motions of normal and abnormal walking in laboratories. The main concern of platform systems is at the prices, familiarity of use, indoor of use. Figure 17 illustrates the foot pressure of the Emed platform.

3.2.2.2 In-Shoe Systems

The in-shoe usually embedded in the shoe [15]. A Commercial one is the Pedar Novel and F-scan system shown in Figure 17.

3.2.3 Sensor Types

3.2.3.1 Capacitive Sensor
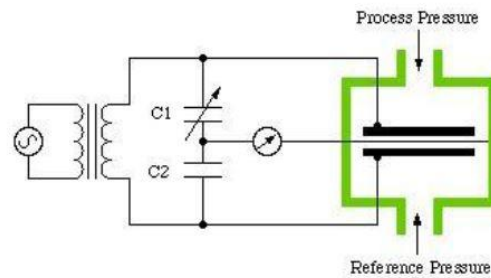
Figure. 18 illustrates the capacitive sensor [15].

It is dielectric elastic consist from two plates and can electricity charged. When the sensor is in charge mode, the two plates will have changed in voltages with respect to the pressure applied. Figure 18 shows the capacitive sensors in Pedar in-shoe.

3.2.3.2 Resistive Sensor

Resistive Sensor is a conductive polymer that modifies the resistance with respect to the force applied between the two electrodes. Figure 19 shows the F-Scan and Tekscan in-shoe system.
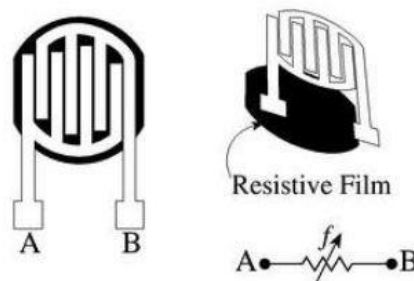
Figure 19 shows the resistance sensors that are commercial in use [15].

3.2.3.3 Piezoelectric Sensors

The Piezoelectric Sensors knew in its high impedance; it also is known as PVDF (Polyvinylidene fluoride).

3.2.3.4 Piezo Resistive Sensors

Piezo resistive Sensor is based on resistance applied. The resistance is high when there is no pressure. When a force applied, there would be changes in the piezoelectric. The adhesive is used together to form the sensor. The commercial one and used in this study is the Flexi-Force sensor from Tekscan USA. It can measure both static and dynamic forces up to 1000 lbf. The active sensing area of the A201 Flexi-Force sensor is 0.375" diameter circle. One method to implement pressure circuit is using an inverting amplifier. The dual line power source inverting amplifier provides a good linearity, and better performance rather than using voltage divider. Figure 20 shows the basic concept of Flexi-Force sensor circuit from Tekscan datasheet.
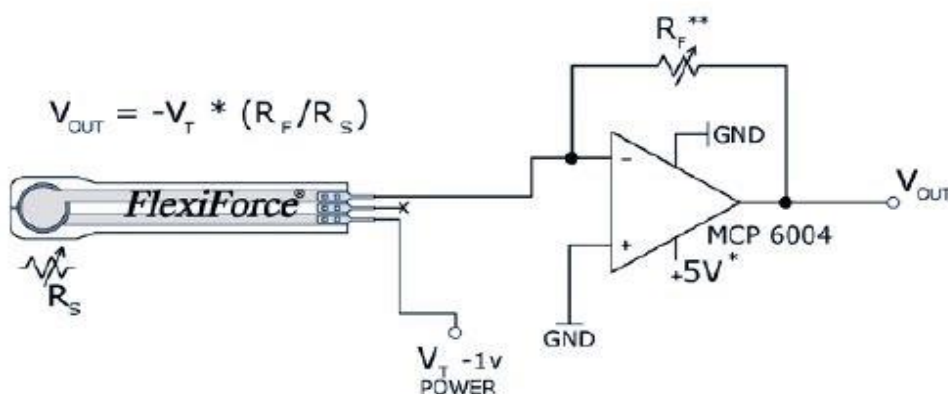
Figure 20 shows the A201 inverting amplifier that uses $-5v$ Dc to output analog signal.

3.3 Flexi-Force Characteristics

The essential role of the pressure sensor is to know the characteristic behaviors. Such as conditioning, saturation, footprint and contact area. Readings may differ if the load distributed over the sensing area. Therefore, it is important to load the sensor and check the load area, whether if it is smaller than or larger than a sensing area of the sensor. If the load is larger than the sensing area, a one may put a "puck" that is a piece of material placed over/under the sensor. The reason is to assure accuracy reading and sensitivity. If the load applied is smaller than sensing diameter, then the load may not place over the edges of the sensor. Flexi-Force sensor is reusable over the time and depends on the application of use. Flexi-Force conditioned over one million load cycle at 50 lb by TekScan's machinary.

3.3.1 Saturation

The sensor can saturate if it worked at the maximum of the recommended range [16]. In the application of op-amp, the refrence resistance (Rf) regulates the sensor sensitvity. Low (Rf) will make the sensor circuit less sensistive, and increase the force range [16].

3.3.2 Conditioning

The condition is helpful to achieve accurate readings. For conditioning the sensor, a one can place 110% of the "test weight" on the sensor to achieve stabilization of reading. If the circuit is configured and calibrated to read up 20N, then the 110% of 20N is 22N. This process has to do four to five times.

3.3.3 Calibration

Calibration is the process of applying a load the same as the load provided during sensor run time. The procedure can be achieved by applying a dead weight and find the sensor resistance (In this study, EZ graph figure 14 is used to measure the forces). The Flexiforce datasheet illustrated the relationship between both the force and the conductance (1/R) as shown in Figure 21.
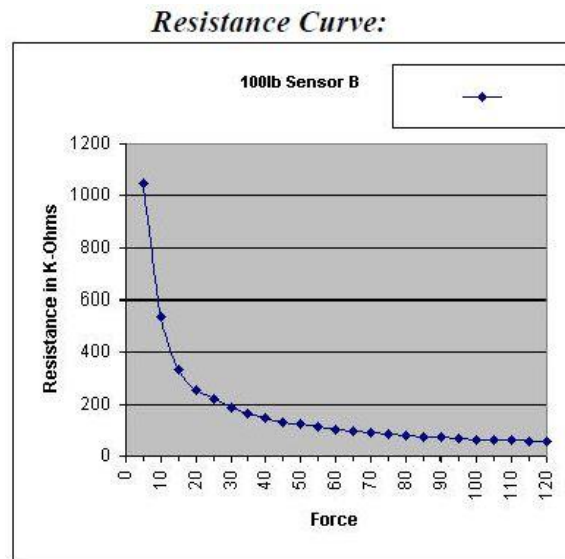
Figure 21 shows the relationship between the force applied and the resistance [16].

However, the sensor should also have to calibrate at the same temperature during run time. Some other aspects may also consider. Like Repeatability in which it is the methods that assure the force repeatedly. Linearity that is the sensor responses to the load. The linearity can control over calibration process. The standard linearity error of the Flexi-Force sensor varies from -3 to +3%. Hysteresis is load unload differences of the full load scale. If the sensor is already

conditioned, the hyhsteresis is blow 4.5% of full scale . The draft is important especially when the sensor is used in different applications. The draft is the variation in sensor output when a fixed load applied over time duration.

3.3.4 Analog Circuit Simulation
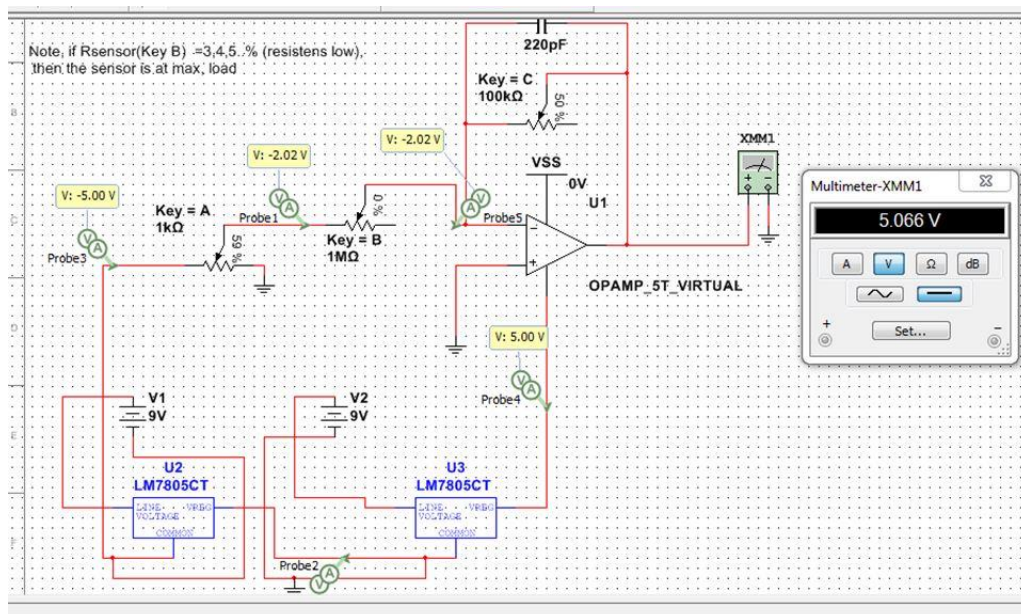
Figure 22 shows the dual line inverting analog amplifier, connected with one potentiometer stands as a Flexi-Force sensor simulated.

With the experimental test using Multisim software, the expected outcomes were the same as the Flexi-Force sensor datasheet. In Figure 22, it shows:

Key A: Stands for R1 resistance (1 Kohm) that regulates the drive voltage (Vt).

Key B: It represents the Flexi-Force sensor assumed one Mega-ohm and descent as the pressure increase.

Key C: It is the feedback resistance from the sensor (Rf = 100Kohm).

The circuit of the system consists of two regulators (LM7805AC microchip) that work on converting $+9v$ and $-9v$ to $+5v$ and $-5v$. The $-5v$ power supply works on feeding the sensor circuit while the $+5v$ is for both amplifier (microchip MCP6002) and Microcontroller Microchip PIC16F688. Both R1 1Kohm and Rf 100 Kohm are the source of adjustment to have an excellent linearity and resolution between the force and resistance. No force applied (Key B, 1 Mohm - 100%), the analog is 0.2. When maximum force is applied (Key B), the voltage $Vout = 5.002v$. Figure 13 demonstrates the outcomes from Flexi-Force sensor characteristic. Where:

Vout = - Vt * (Rf/R_Sensor).

The A201 FlexiForce linearity, Repeatability, Hysteresis, Drift, and Response time concluded from the table below [16].
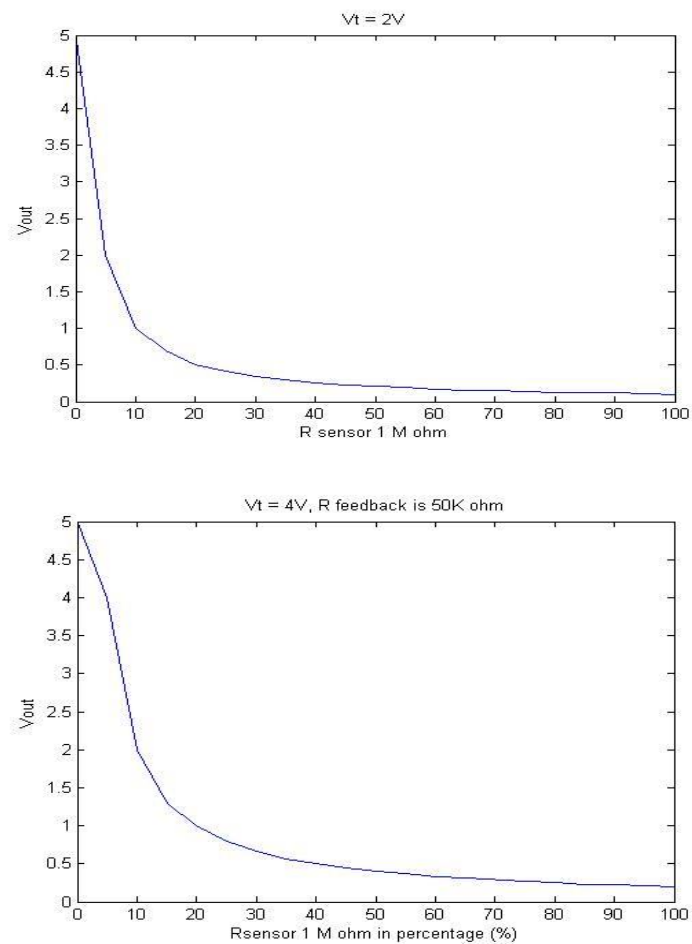
Figure 23 the actual sensor responses with respect datasheet in figure 21

STANDARD FLEXIFORCE SENSOR (MODEL A201)

Thickness	0.008 (0.208 mm)
Length	8" (203 mm) 6" (152 mm) 4" (102 mm) 2" (51 mm)
Width	0.55" (14 mm)
Sensing Area	0.375" (9.53 mm) diameter
Connector	3-pin male square pin (center pin is inactive)
Force Ranges	0-1 lb (4.4 N) 0-25 lbs (110 N) 0-100 lbs (440 N)*
Operating Temperature Range	15°F to 140°F (-9°C to 60°C)
Linearity (Error)	+/- 3%
Repeatability	+/- 2.5% of full scale (conditioned sensor, 80% force applied)
Hysteresis	<4.5% of full scale (conditioned sensor, 80% force applied)
Drift	<5% per logarithmic time scale (constant load of 90% sensor rating)
Response Time	<5 microseconds
Output Change/Degree F	Up to 0.2% (~0.36% / °C). Loads <10 lbs, operating temperature can be increased to 165°F (74°C).

Table 1 shows the characteristics specifications of A201 Flexi-Force from TekScan.

* Where 0-25 lbs is considered low force range, and 0-100 is considered a high range.

3.4 System Circuit

The wearable prototype system as mentioned above is a dual line circuit power. It can provide the most versatility in terms of force range adjustment. The circuit later converted to work with only one power source using LT104 chip converter. The system used to sum the sensors with invertible amplifier shown in figure 24 rather than using voltage divider in related studies – that discussed in the previous chapter. Six sensors tested and placed according to foot structure distribution. However, these six sensors are subject to place and remove base on a user need. Sensors positions depend on the related variables the author would like to achieve. One way to

measure the footstep pressure area is by the imprint tool that uses the ink to determine the pressure area of the foot.

The analog voltage can determine as:

$$Vout == -Vt \left(\frac{Rfeedback}{Rsesnor}\right), \text{ where } Vt = +5 \left(\frac{RSensor}{R1+Rsensor}\right),$$
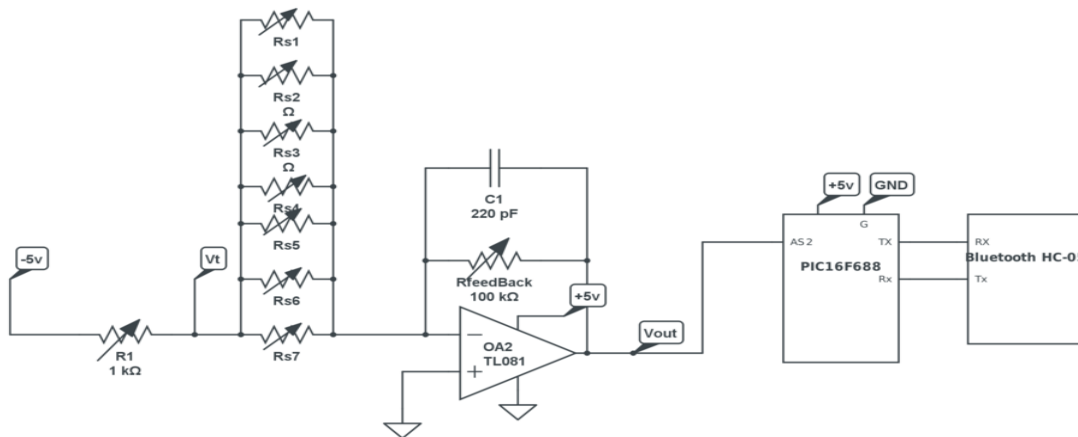
Figure 24 demonstrates the system circuit used six sensors summed with invertible amplifier and data acquisition.

Therefore: $Vout = 5v\left(\frac{Rfeedback}{Rsensor+R1}\right)$

Hence, the circuit uses the pressure sensors in parallel for six A201 sensors, but the sensors are sharing the same voltage input, therefore the final output explained below.

If a one assumes taking three sensors in parallel, then the equation would be: -

$$Vout = \left\{ -\frac{Rf}{Rs1||Rs2||Rs3} \right\} * Vt$$

$$Vt = V_{source} * \left\{ Rs1 \frac{||Rs2||Rs3}{R1 + (Rs1||Rs2||Rs3)} \right\}$$

$$Vout = Vsource * \left\{ -\frac{Rf}{R1 + (Rs1||Rs2||Rs3)} \right\}$$

.

.

.

$$Vout = Vsource \left(-\frac{Rf}{R1} \right) \left(\frac{1}{1 + \frac{1}{R1}(Rs1||Rs2||Rs3)} \right)$$

$$Vout = Vsource \left(-\frac{Rf}{R1} \right) \left\{ 1 + \frac{1}{R1}(Rs1||Rs2||Rs3) \right\}^2$$

The final output voltage (Vout) ranges from 0-5v represents the force from the foot. Section 3-5, will discuss the linear model further. A system designed to use Flexi-Force A201 sensors joined in parallel, and the analog output is proportional to the sum of the input gain. The gains from the three sensors are the one input channel in the microcontroller. (specifically channel RA2). PIC16F688 microcontroller 10-bit A/D converter used to convert and transmit 100 Hz via serial port UART (Rx-TX, TX-Rx).

This model is conditioned and calibrated to maintain precise results, and to mitigate the effects of drift and hysteresis by using EZ graph Shimadzu at Dr. Xuejun Wen's lab, department of

chemical and life science engineering. Each sensor conditioned four to five times by placing 110% of the test weight on the sensor. Furthermore, a statistical analysis T-test between each two sensors used to determine the variances and significance differences between the sensors. Table 2 demonstrates the calibration of eight individual sensors. The output observed concludes the good quality assessment for sensor measurement.

Newton	Sensor1	Sv1	Sensor2	Sv2	Sensor3	Sv3	Sensor4	Sv4	Sensor5	Sv5	Sensor6	Sv6	Sensor7	Sv7	Sensor 8	Sv8
100	185	0.88	167	0.81	169	0.82	178	0.86	165	0.8	200	1.02	213	1	178	0.81
200	395	1.91	345	1.67	409	1.99	368	1.79	347	1.68	423	2	403	1.94	346	1.67
300	602	2.92	508	2.46	644	3.12	567	2.75	508	2.47	613	2.92	576	2.78	500	2.41
400	795	3.85	655	3.16	873	4.23	743	3.6	670	3.25	775	3.7	738	3.53	646	3.11
500	960	4.65	795	3.82	1021	4.95	902	4.36	822	3.98	922	4.4	885	4.24	774	3.74
600	1022	4.95	920	4.43	1021	4.95	1022	4.95	946	4.59	1022	5.95	1011	4.89	897	4.33
Mean	659.84	3.193	565	2.72	689.5	3.343	630	3.05	576.33	2.795	659.16	3.35	637.68	3.065	556.8	2.6
Str.	328.171		281.80		347.88		321.7		294.02		310.76		299.95		269.2	

Table 2 shows the output readings from each sensor measurements in both analog and digital microcontrollers.

The statistical analysis for the T-test – two samples assumed unequal variance showed that with a confidence interval 95% no differences between Sensor1 and Sensor2 (Figure 15). Similar

results for rest of sensors maintained with a P-value > 0.05. Force sensors calibrated up to 600

N/cm^2 for the T-test. An example for T-Test hypothesis of the first two sensors:

First, taking S1, S2 and apply T-test for two samples: -
Assume -
$\mu o = 0$ $Null\ hypothesis.\ there\ is\ no\ difference\ between\ S1\ and\ S2.$
$\mu 1 \neq 0.\ Alternative\ hypthesis.\ We\ calim\ that\ there\ is\ a\ difference.$

Second, determine T- test by the following equation:
$T = \frac{mean\ of\ X1\ - mean\ of\ X2}{\sqrt{S1^2/n1+S2^2/n2}}$

Where S1, S2 are the standard dev. $= \sqrt{\frac{\in(di-D)^2}{n-1}}\ for\ each\ S.$
T = 0.53701 (By Finding this value from the table, using degree of freedom and alpha value).
Then apply P-value= 2*(t>T).
Assume confidence interval is 95%, so alpha is 0.05. Since P-value>alpha.
It means fail to reject the null hypothesis. There is no significant difference between S1 and S2.

t-Test: Two-Sample Assuming Unequal Variances

	Sensor 1	Sensor 2
Mean	659.8333333	565
Variance	107696.5667	79415.6
Observations	6	6
Hypothesized Mean Difference	0	
df	10	
t Stat	0.537014024	
P(T<=t) one-tail	0.301500237	
t Critical one-tail	1.812461123	
P(T<=t) two-tail	0.603000475	
t Critical two-tail	2.228138852	

Figure 25.a shows the results of T-test table of first two sensors.

Where *the P value* $= 0.603$ is greater than the confidence interval (Alpha). However, the model was readjusted to read up to 1000KPa, 100N/cm^2.

A further development on the hardware of the circuit done by adding the LT1054 switched capacitor voltage converter with the regulator. The chip was able to produce 53mA power supply and convert the $5v$ to $-5v$ to supply the sensors. LT1054 can supply higher current and lower voltage loss.

Chip Converter LT1054	
R1	20Kohm
R2	100Kohm
Cin	$10\mu F$
Cout	$100\mu F$
C1	$0.002\mu F$
MCP6002 Chip amplifier.	
R_feedback	200Kohm
Rs	Flexiforce sensors.
R1	85Ohm
C1 (Capacitor in parallel with R_feedback)	220pF
Microcontroller used	PIC16F688
Bluetooth module	(Rx-TX connection) HC-05

Typical Application
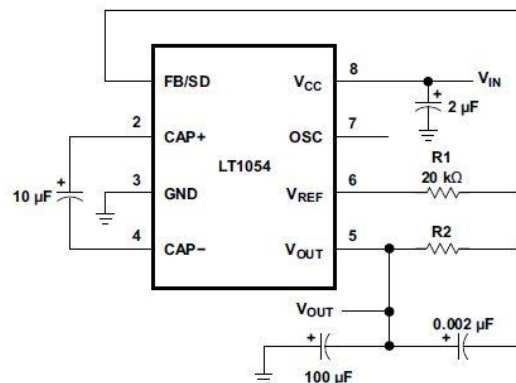
Figure 25.b shows the components used in sensors circuit

LT1054 chip converter used to supply $-5v$. The final circuit design illustrated in Figure 25.c. The voltage drop is estimated $1.1v$ while the supply voltage is from $3.5\ to\ 15v$. the chip has an FB/SD to regulate shutdown for low current operation at pin 1 and to regulate the voltage output. The basic voltage inverter/regulator for the LT1054 shown in the Figure 25.c. The overall schematic of the circuit shown in the figure 25.c.
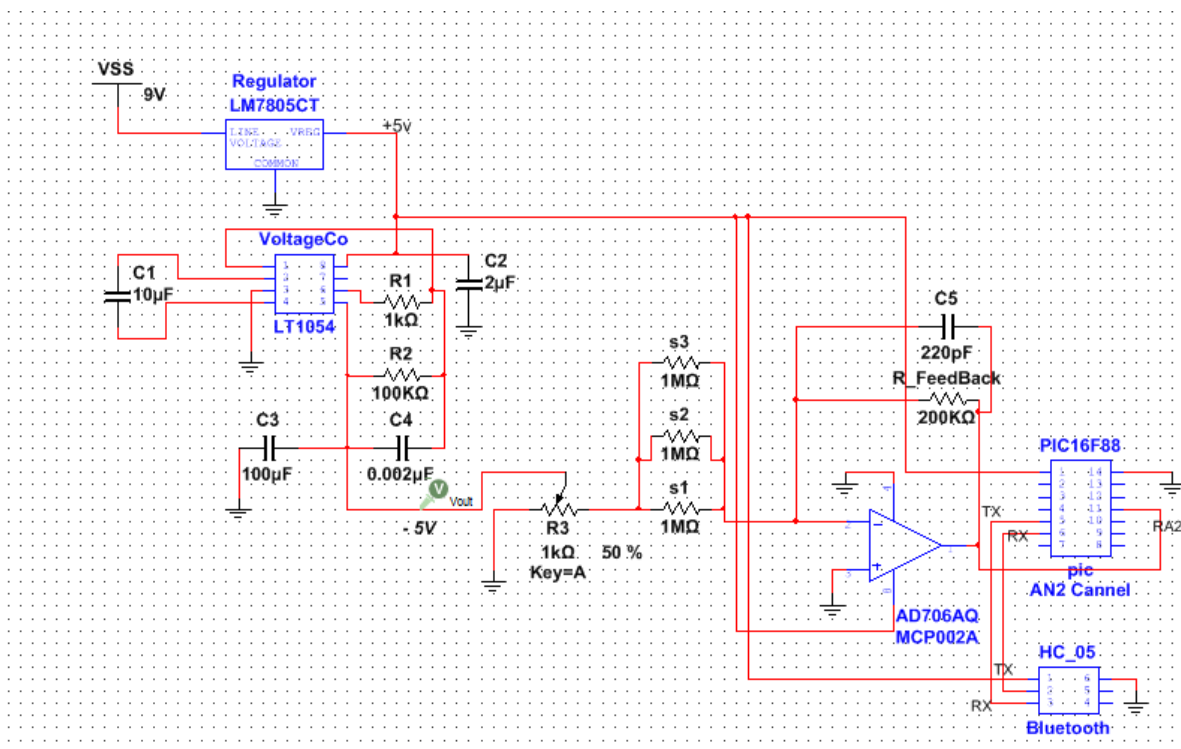
Figure 25.c. shows the final design for the circuit system used LT1054 voltage converter instead of the dual line power supply at figure 22.

3.4.1 PCB

A printed circuit board built to be the fit model for the circuit after mentioned in figure 25.c. Altium Designer 15.1 is used to design the schematics and the PCB with a two-layer base. Two by two inches, and name it Plantar 1.0. A polygon pours utilized to fill out all the spaces with a copper at the top layer and bottom layer. In which the clearance to have enough spaces for soldering between the copper and the components is 20 mil. Gerber files and NC drill files built to be ready for fabrication. Figure 25.d and figure 25.e show the final design of circuit semantics, PCB design, and size.
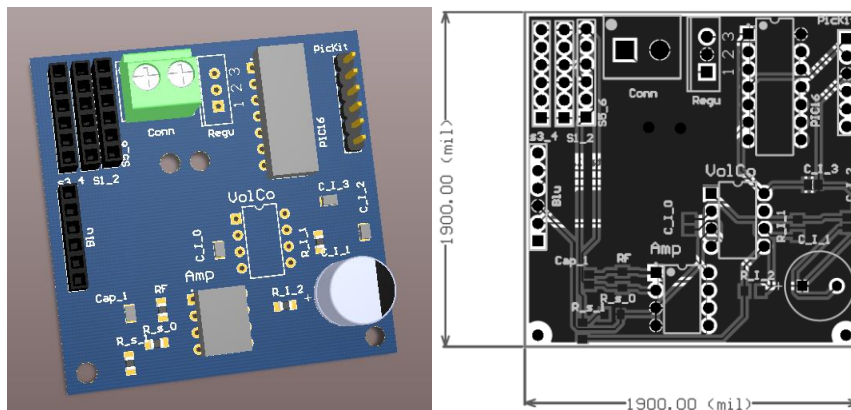
Figure 25.d shows the PCB physical size and design
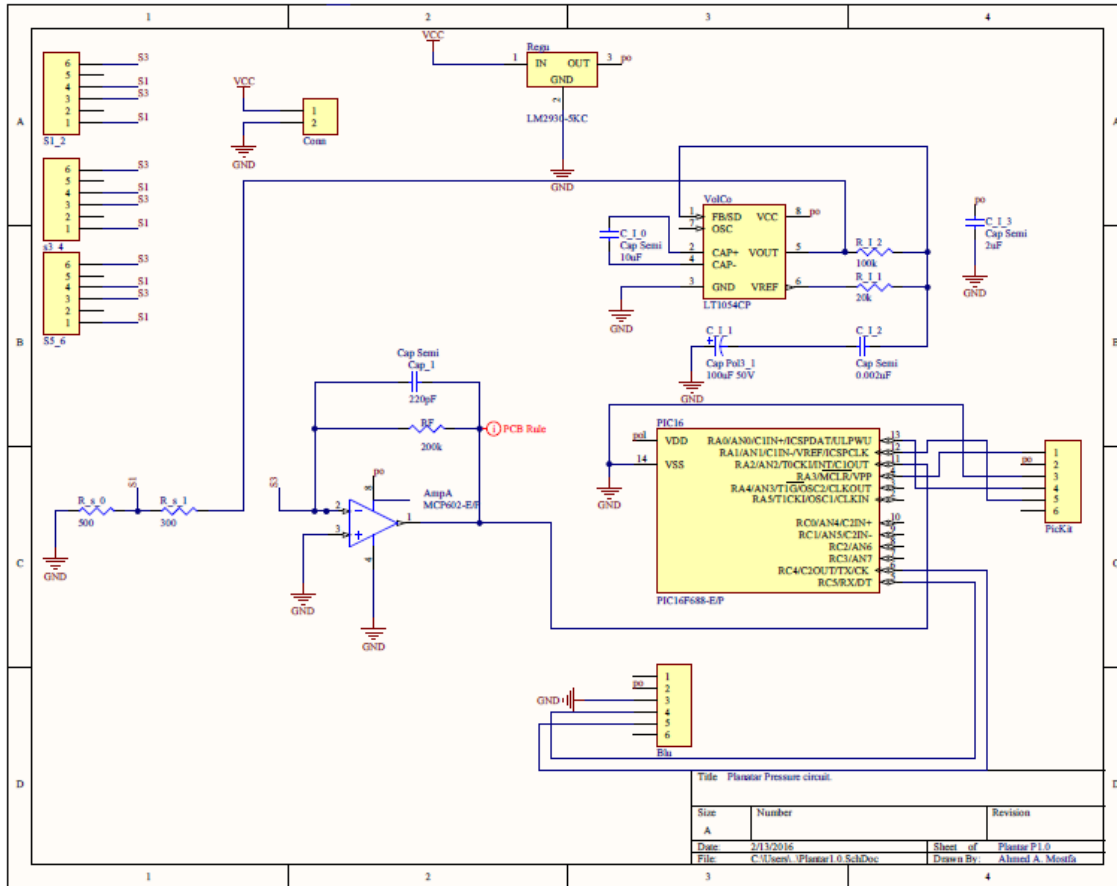
Figure 25.e shows the system schematics in Altium designer

3.5 Linear Regression Relations

The sensor resolution shows the outcome when adjusting the Trim Pot of the drive voltage Vt with Rf fixed at $50\ Kohm$. The left chart shows resoultions of the sensor outcome when varying the Rf ($R\_feedback$) with fixed Vt at $-3v$.

Adjusting full scale force range with V$_T$ Trim Pot
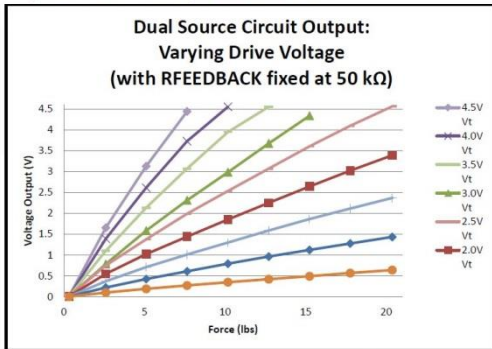
Adjusting full scale force range with R$_{FEEDBACK}$ Trim Pot
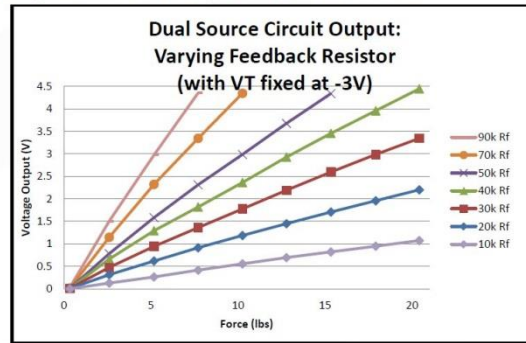
Figure 26 shows the resolutions of the sensor [16].

The model was readjusted to read up to nearly 1000KPa- 100N/cm^2. Rather than different studies discussed in the next chapter. However, the pressure sensor can appear in millibars (mbar), other measurements can be in inches of mercury (inHg). Units of pressure concluded as 1 mbar (millibar) = 0.001 bar = 0.1 KPa (Kilopascal) = 1 hPa (hectopascal) = 1000 cm^2 (dynes per square cm) = 0.000987 atm (atmospheres) = 0.0295 inHg (inches if mercury) = 0.750 mmHg (mm of mercury) = 0.0145 psi (pound per square inch) [17]. To get excellent linearity readings based on the desired force applied, adjusting full scale in both force range with voltage drive (Vt) and force range with R feedback (Rf) Trim Pot [18], as shown in Figure 26.

Linear Regression applied to represent the force in Kilo-Pascal ($where\ 1\ pascal = 0.0001\ N/m^2$).

The process of linear regression is done by applying certain weight from EZ-Graph to the A201 Flexi-Force sensor and since the microcontroller is 10-bit ADC, then the maximum value can read is 1024 as illustrated in the table below.

Force Applied	Digital o/p	Analog o/p
10	15	0.09
20	112	0.55
30	234	1.112
40	360	1.76
50	480	2.334
60	618	2.998
70	740	3.58
80	867	4.197
90	1000	4.835
100	1023	4.942

Table 3 shows the forces applied from EZ-Graph on the A201 Flexi force sensor to determine

both readings analog and the digital one.

The linear regression can conclude in the equation below

$y = Bo + B1x + \in$ (If we increase x by 1 unit, y will increase by B1).

Y= is the dependent variable (y-axis) response.

X=independent variable (predictor).

Bo is the y-intercept

B1 is the slope.

$B1 = \frac{\sum(x - mean\ of\ x)(y - mean\ of\ y)}{\sum(x - mean\ of\ x)}$

Bo = is the intercept that can derive from y=Bo+B1x.

$R^2 = \frac{\sum(estimated\ value\ of\ y - mean\ of\ y)^2}{\sum(y - eatimated\ vaule\ of\ y)}$

E is the residual (error). $\in = yi - \gamma i$.

The simple model result by Microsoft-Excel from Table 3 is:

$$y = 9.677 + 0.0831 * x$$

Where x is the digital value (Predicted – independent input), and y is the dependent variable.

That will get the value in Newton. Where $1\ Newton/\ cm^2 = 10\ Kilopascal. Then\ y = y *$

10. Results of the linear regression from Excel are demonstrated below Figure 27 and 28

54
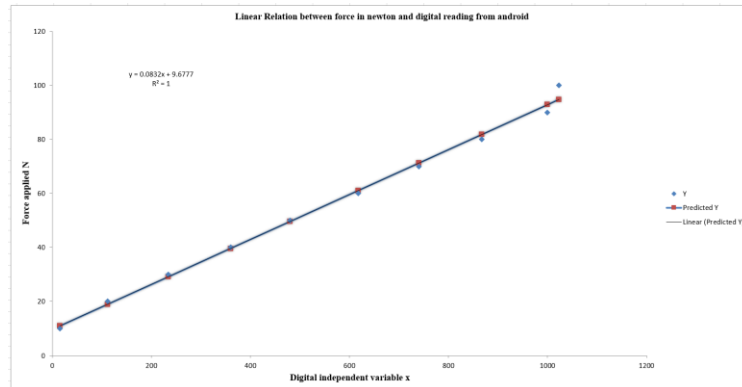
Figure 27 shows the dependent and independent variable of the linear regression.

Since the model used in this study is a combination of multiple forces distributed around the foot area. The force, for example, that causes a force of 40 N total may come from the first sensor that is in the heel area. Alternatively, that pressure may result from two sensors distributed across two different areas. Therefore, a person cannot predict where that combined force came from. Hence, it is a combined force and each sensor may rely on each other, a single simple linear regression model can represent these forces. To justify that. A correlation coefficient calculated to see if there was a strong relationship between the sensors distributed around the foot area. We assumed that since there was a strong relationship between the sensor readings. In which the sensors were tested in the table below, a simple model can utilize and the forces from the sensors can combine as one input.

Force (N)	Sensor_3		Sensor_5		Sensor_6		Sensor_7		Snesor_8	
	Voltage output	Digital output	Voltage output	Digital output	Voltage output	Digital output	Voltage output	Digital output	Voltage output	Digital output
10	0.68	216	0.255	140	0.73	224	0.16	126	0.67	214
20	1.16	298	0.63	208	1.497	359	0.552	195.5	1.28	320
30	1.75	402	1.024	275	2.28	492	1.088	288	1.78	404
40	2.31	500	1.561	367	3.214	655	1.68	387	2.34	410
50	3.04	620	2.03	446	4.12	806	2.315	501	3.0	597
60	3.59	716	2.55	536	4.93	946	2.98	614	3.47	648
70	4.1	820	3.05	626	4.93	946	3.65	730	4.28	721
80	4.8	930	3.577	717	4.94	946	4.32	846	4.93	854
90	4.91	946	4.22	826	4.94	946	4.93	946	4.93	946
100	4.91	946	4.78	927	4.94	946	4.93	946	4.93	946

Table 4. Shows the experimental results for five sensors tested to measure the correlation

coefficient between each others.

Correlation coefficient ranges between +1 to -1. A positive correlation is when the R result is

close to one. While a weakness correlation between two sensors expresses when it is close to

zero. -1 represents a negative correlation between two sensors. MATLAB 2011.a used to test

correlation coefficient, where the results are shown below.

The results coefficient correlation between the sensors explained that a simple linear regression

model could express the forces distributed around the foot. Where the results show that there

is strong correlation coefficient (close to 1) between sensors tested in table 4. That justifies

why we didn't go through multiple predictors. I.e. multiple linear regression.

So, the model can write:

$y = b_0 + b_1 x$. Instead of multiple independent predictors.

If and only if there is a weakness correlation between two sensors, a one can add its predictor

as illustrated below – to be multiple linear regression.

$$y = b_0 + b_1 + b_2 x_2 + b_3 x_3 + ...$$

The correlation coefficient between sensors to fit the model.

- s3 = load('s3.txt');
- s5 = load('s5.txt');
- corr_sensor_3_5 =corr2(s3,s5);
- s6 = load('s6.txt');
- s7 = load('s7.txt');
- corr_sensor_6_7 = corr2(s6,s7);
- s8 = load('s8.txt');
- corr_sensor_7_8 = corr2(s7,s8);

corr_sensor_3_5 = 0.976.

corr_sensor_6_7= 0.922.

corr_sensor_7_8 =0.994.

SUMMARY OUTPUT

Regression Statistics	
Multiple R	0.997310084
R Square	0.994627404
Adjusted R Square	0.99395583
Standard Error	2.353824383
Observations	10

ANOVA

	df	SS	MS	F	ignificance F
Regression	1	8205.676	8205.676	1481.038	2.28E-10
Residual	8	44.32391	5.540489		
Total	9	8250			

	Coefficients	andard Err	t Stat	P-value	Lower 95%	Upper 95%	ower 95.0%	lpper 95.0%
Intercept	9.677685881	1.393194	6.946402	0.000119	6.464975	12.8904	6.464975	12.8904
X Variable 1	0.083175471	0.002161	38.48426	2.28E-10	0.078192	0.088159	0.078192	0.088159

RESIDUAL OUTPUT

Observation	Predicted Y	Residuals
1	10.92531795	-0.92532
2	18.99333863	1.006661
3	29.14074608	0.859254
4	39.62085542	0.379145
5	49.60191194	0.398088
6	61.08012693	-1.08013
7	71.22753438	-1.22753
8	81.79081919	-1.79082
9	92.85315683	-2.85316
10	94.76619266	5.233807

Figure 28 demonstrates the Excel output from linear regression

Regression shown has R_Square very close to one (0.9946, good to fit, and it explains that around 99.46% of the output (y) can be explained by linear relationship regarding the input x), and the Mean Square Residual (MSE) is 5.5404.

The statistical analysis gave us some conclusions:

- The reliability of the sensor used in this model, by performing T-test for each two sensors and showing that there is no significance difference between the two sensors and so on for the rest.

- It gave us the linear equation, from digital readings, - that represent the force in Newton (Multiple by 10 to be in Kilopascal).

- The system model is now able stimuli between the ranges of 100KPa to 950KPa.

Chapter 4 Android IDE Platform Implementation and data analysis

Android studio is the integrated development environment IDE. It used in this study to provide a user-friendly interface in which it has therapeutics features in both temporal and spatial parameters. Android app is written in Java programming language. The Android SDK are the tools compile of the code. Before going through the details of app use, it is important to introduce the essential parts of Android life cycle programming that are the base of establishing the first app. Through the life cycle of the app code development, the app goes through a sequence of the pyramid in which the activity can occur, as shown in figure 29. The system may leave one of the method activities within the life cycle like $OnStart()$ method, and gets back to it due to the complexity of the app features [19].
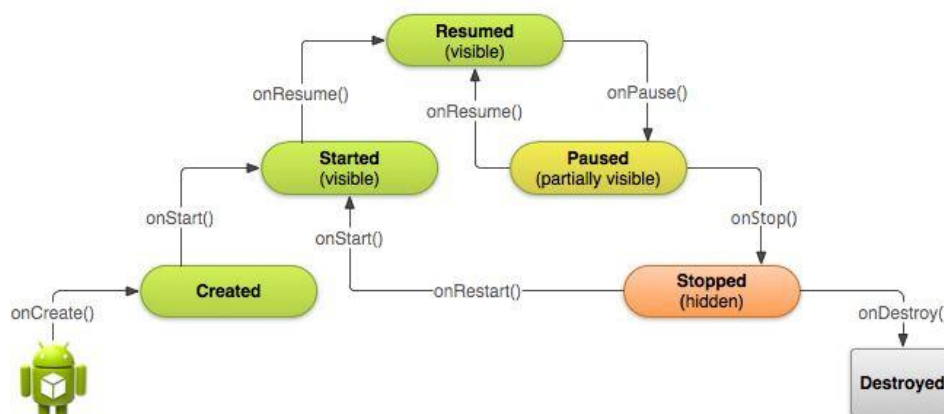
Figure. 29 demonstrates the pyramid life cycle activity of any Android app with the callback methods [19].

However, the concepts of understanding the life cycle methods are:

1- To prevent system crashing.

2- To not consume system resources.

3- To not block the main thread of the system and slow down the app performance.

At $onCreate()$ method, a user can declare the user interfaces for the app's functions. Like $TextView$, $Button$, $ListView$, and etc. In addition, it can define variables and configure user interface UI [19]. Once the $onCreate$ method finished, the system would call $onStart()$ method and $onResume()$ method.

The system would call $onDestroy()$ method after $onPause()$ and $onStop()$ methods already created. $onDestroy()$ is usually called to kill the app after use. In this study, the Android used API 21 version 5.0.2 Lollipop. According to Android Dashboards, 16.3% of Android devices distributed were running on this particular platform.

4.1 Plantar Pressure App Features.

4.1.1 Bluetooth Connection.

Since the system circuit in this study requires Bluetooth module (HC-05 Bluetooth) connection, the app first has to have system permission for use Figure 30:

```
<manifest                                    ...                                    >
    <uses-permission        Android:name="Android.permission.BLUETOOTH"        />
                                                                                ...
</manifest>
```

Figure. 30 shows Android system permission at the manifest file to use Bluetooth device [19].

The app slave side has to:

1- Scan for other Bluetooth devices.

2- Query the local adapter (Permission to pair devices).

3-Build RFCOMM channel and transfer the data.

The java ME programming in Android studio for Bluetooth starts by acquiring $BluetoothAdapter$ class. The Android devices usually have only one Bluetooth adapter for the system. Once that is done, a request to enable Bluetooth would appear as a dialog message and would call $startActivityForResult()$.

Next is finding devices by scanning local area for Bluetooth enabled. If that Bluetooth device is in discoverable mode, it will share information like MAC address and device name [19]. But before that, the both devices have to agree (paired key) in order to establish the connection, and that can be done by calling $getBondedDevices()$.

In terms of discovering devices, it would simply call the method $startDiscovery()$

This process will automatically begin looking for local devices in which it will cost many system resources . Searching for these local devices will take 120 seconds [19]. Hence, once a device found and connected, it has to call $cancelDiscovery()$ before connection starts.

There is a difference between paired and connected devices. Paired devices mean that the devices know each other and share the key for authorization. Connective devices mean that the devices are sharing RFCOMM and are able to transmit the data.

To connect two devices, one must be a server and another one should be the client. That would have performed by calling $BluetoothServerSocket()$ that works on Service Discovery Protocol SDP in which it includes the UUID that is the base of connection agreement [20]. The UUID is Universally Unique Identifier that has 128-bit format to identify the information

(Application's Bluetooth Service) [19][20]. A one can introduce and generate UUID from citation provided [21]. When Bluetooth connection gets $aceept()$, the $BluetoothSocket$ is acquired. In here, transferring the data occurs, and it can done by using $InputStream$ and $OutputStream$ to handle the data transmitting through the socket, also by using $read(byte[\,])$ and $write(byte[\,])$. a one can refer to Android Bluetooth documentation provided at the after mention cited for more information and codes.

4.1.2 MP Android Chart.

This study used one of the powerful Android chart views, graph view by Philip Jahoda [21] and examples implementations by Mohit Gupt [22]. It can support line, pie charts with features like zooming in/out, dragging, animations, fingerprint etc. It is one of the libraries that are available online and falls under Apache 2.0 license. It can support -

1-Simple Bar Chart

2- Horizontal Bar Chart.

3- Simple Line Chart.

4- Line Chart with Cubic Lines.

5-Pie, Scatter, and Radar chart.

During the study, the plantar pressure app passed through certain libraries until it ended up choosing an efficient library that is MP Android Chart Figure 31. The previous libraries used are Graph view by Jonas Gehring and AChartEngine library supported from 4ViewSoft Co. It discovered by the time that they do not have the enough features as MP Android Chart line in which it has zooming in/out etc [23].

Figure 31 shows the app development for chart line library and features.

The features used in this app are Splash screen with University logo. MP Android chart line is shown at lower right corner.

4.2 SMA and signal recovery.

As mentioned in chapter 3, the system circuit consists of three sensors summed with one amplifier and with dual line circuit and connected with the PIC16F688 Microcontroller that works on converting the gain summed from three sensors distributed around the foot area of the heel, midfoot and metatarsal. The microcontroller ADC 10-bit embedded code works on converting $from\ 0\ to\ 5\ volt.$ $In\ which\ it\ represents\ from\ 0\ to\ 2^{10} = 1024\ in\ digital\ form.$ Since there is no significant difference between sensor and sensor in

digital output (T-test), one predictor was chosen to represent the linear regression as its shown in table 3 and Figure 27. The linear equation converted later to be in Kilopascal within the range 100KPa to 950KPa.

As shown in Figures 24, the analog signal successfully converted to be represented in digital form. Plantar pressure app with a frequency programmed in 100Hz retrieved the analog signal in the same shape after applying SMA with window size 4. The test is done for two subjects with normal walking speed and six sensors distributed. Simple moving average was applied and compared with the original signal to see what efficient window size is close to the reality of original signal.

SMA effectiveness

SMA with window size 10.

SMA with window size 2
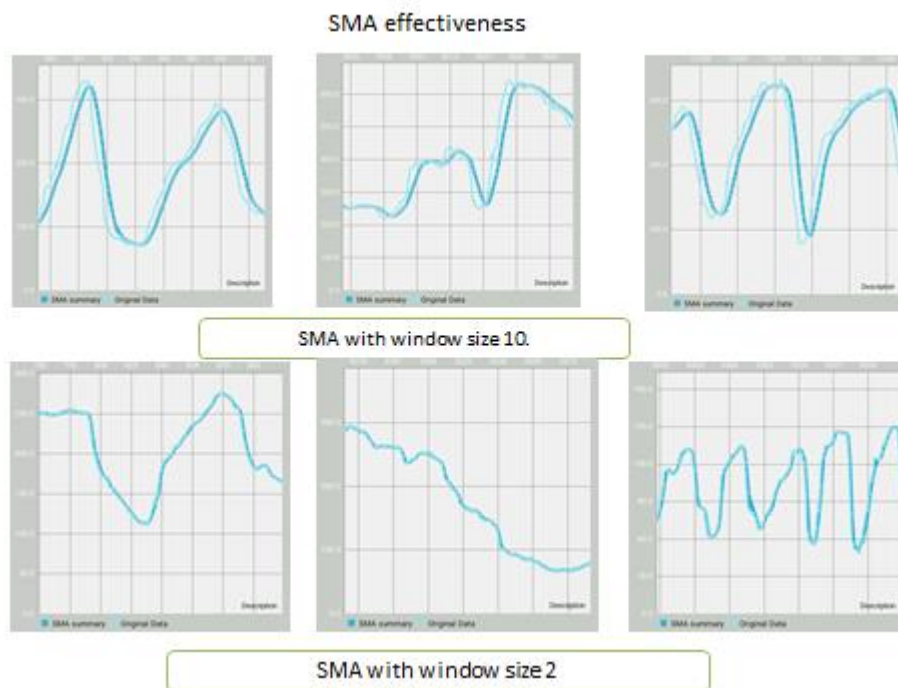
Figure 32 shows the simple moving average applied and compared with the original signal to smooth the chart line.

This type of method helps to filter the noise from the random signal fluctuating. Simple moving average first applied in Matlab to see the effectiveness and difference with the original signal before implementing the Android java code.
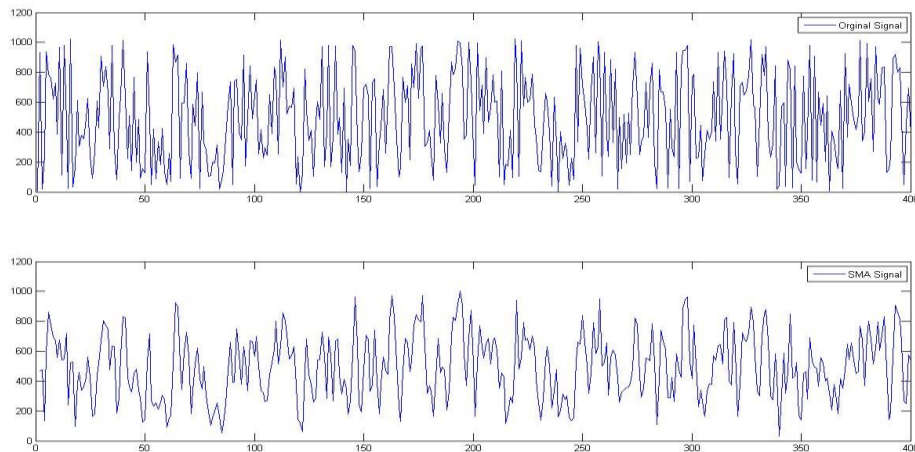
Figure 33 shows the result of 400 samples varies from 0 to 1024 with window size 2 to show the effectiveness of SMA.

```
x = randi([0,1024],1,400);
t = tsmovavg(x,'s',2);
subplot(2,1,1);
plot(x);
legend(Original Signal')
subplot(2,1,2)
plot(t);
legend('SMA Signal')
```
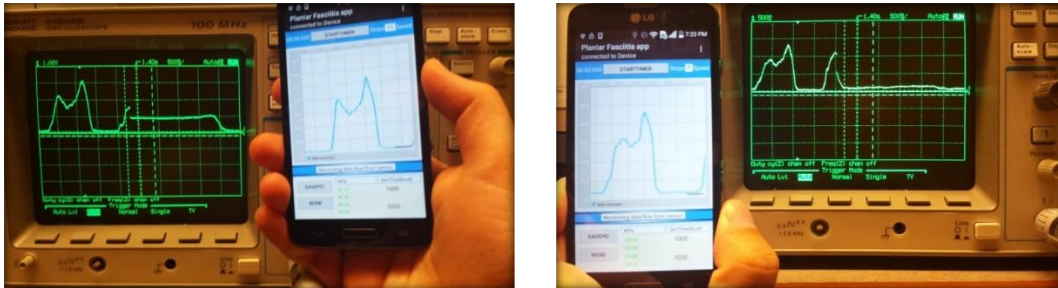
Figure. 34 shows signal recovery with sampling frequency 100Hz for two male subjects with normal walking and six sensors.

Signals from each area of the foot also studied to show the best placement position. More than two trails performed for each individual try and test. In order to come up with the right shape of foot contact area in which they knew at figure 2. The first trail was started by placing only one sensor at the heel contact. After then mid-foot, metatarsal, and great-toe were also tested. The results are shown in figure 35. The interpretation of the figures with several trials tells that the Flexi-Force sensor calibrated to be sensitive to each of the contact area and calibration have done for such purposes. Where these sensors calibrated to read up $100 - N/cm^2$ for each sensor. The sensitivity of sensors and high resolution discussed previously by using circuit resistance/potentiometer for $R\,Feedback$ at the amplifier and $R1$ that regulates the voltage output to the sensors.

Figure.
Sensor distribution with Parotec insoles (Paromed GmbH, D-8201, Markt Neubeuern, Germany). LH = lateral heel, LM = lateral midfoot, MH = medial heel, MM = medial midfoot, M1 = 1st metatarsal head, M2–3 = 2nd to 3rd metatarsal head, M4–5 = 4th to 5th metatarsal head.
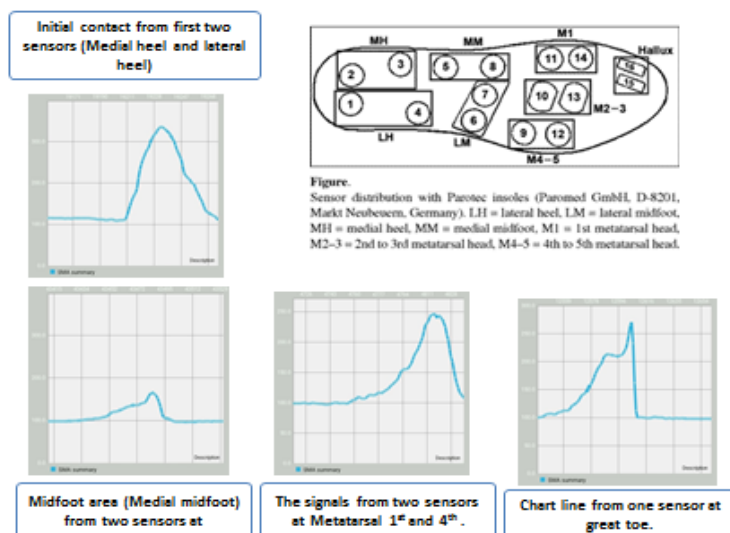
Figure 35 shows the sensor effects at each area of the heel, midfoot, and metatarsal for testing and finding best graph shape.

In addition to that, two sensors were placed at the heel and metatarsal head 1st. One subject (26

Figure 35.a shows the two sensors placed at the heel and 1st metatarsal of the left foot.

age, and 175 cm) walked normally for 100 steps in a straight floor with a fairly 1 minutes and 20 seconds as a first trial shown in figure 35.a. The second trail involved determining the peaks during the normal walking for the same subject. The subject walked for 92 steps for about 58 seconds and 177 milliseconds. The peaks were determined in Android as shown in Figure 35.b.
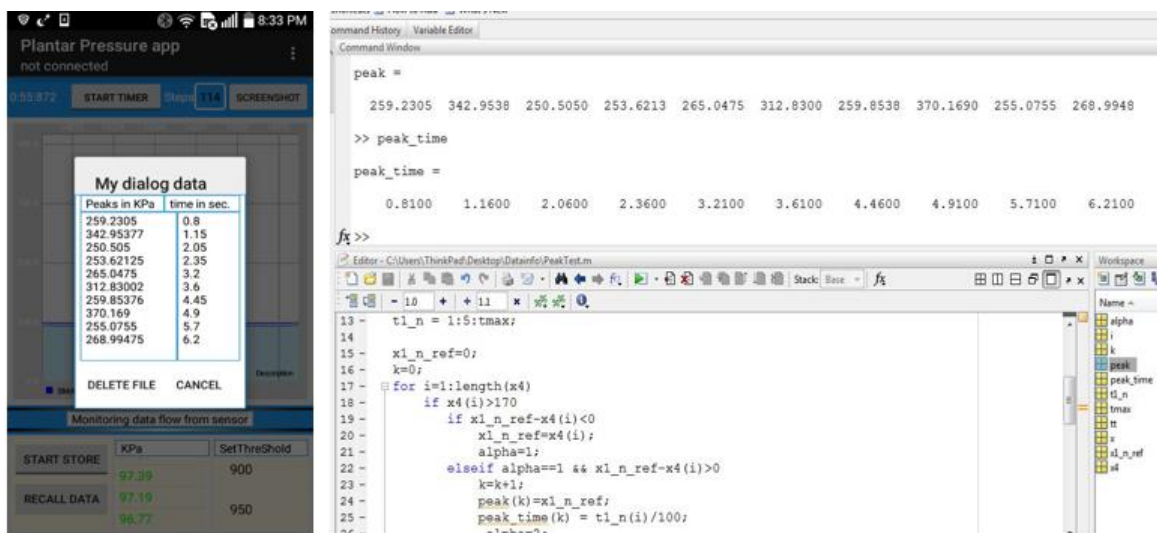
Figure 35.b system records and graphs for two sensors and peaks in both Android and MATLAB algorithm.
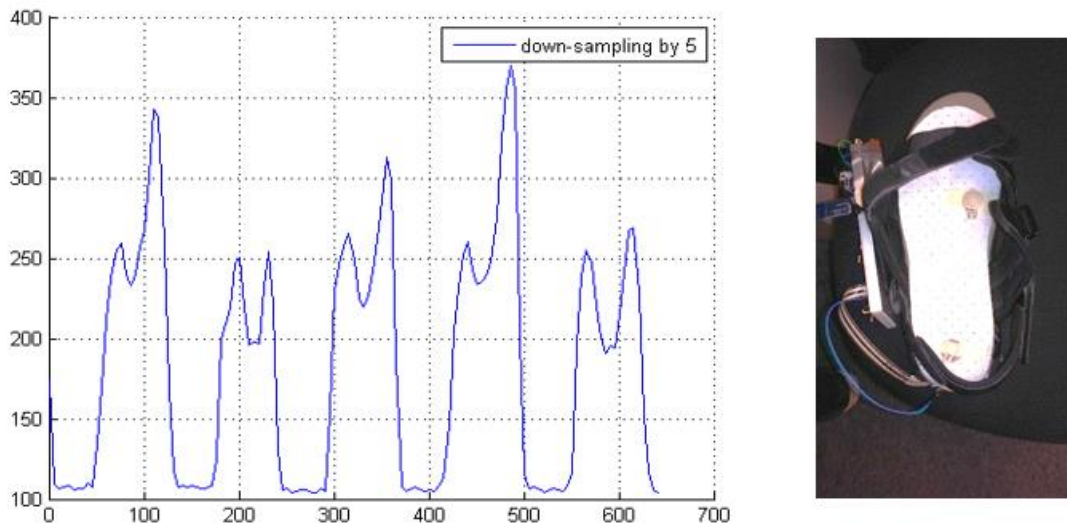
Figure35.c demonstrates the system results of the trail2 recorded while normal walking and with the two sensors at the heel and 1st metatarsal.

It is worthy to mention that both algorithms determination in MATLAB 2011.a. and Android app algorithm is working efficiently. It tells nothing but the reliability of the system. One of the features in the Android app - in addition to screenshot, one-hour timer toggle button, step counter, clean graph, and share data – is cleaning the records from the file recorded. It would be no means if the same file still exists to record on it again. Therefore, a delete button introduced in java Android ME to delete the entire file and peak records.

The Pathological and therapy departments are interested in finding some parameters like time to peak (In which it is the first peak occurred) and peak-to-peak time. Figure 35.c shows the graph outcome from the two sensors mentioned above.

Signal summary from five sensors placed according to pathological studies.
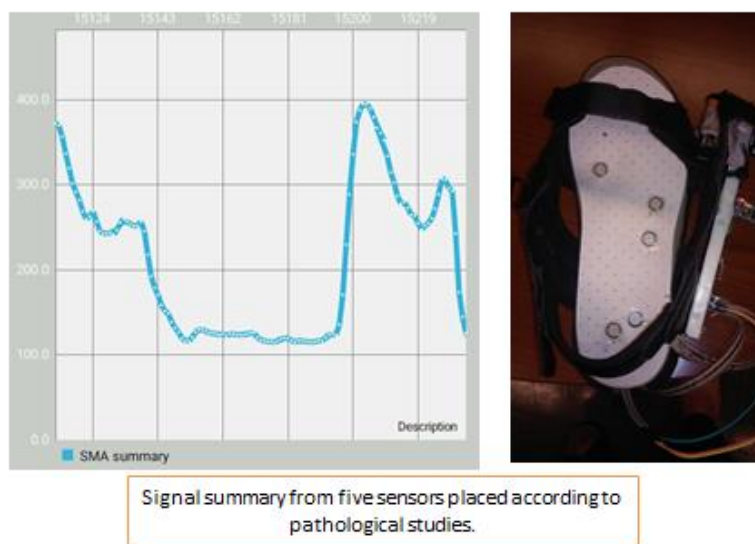
Figure 36 shows the in-shoe system circuit with a testing five sensors at the right foot.

Signal summary of six sensors. Notice that the smoothing signal and placing the sensors can play essential roles to obtain the camels one valley of the Gait Cycle.
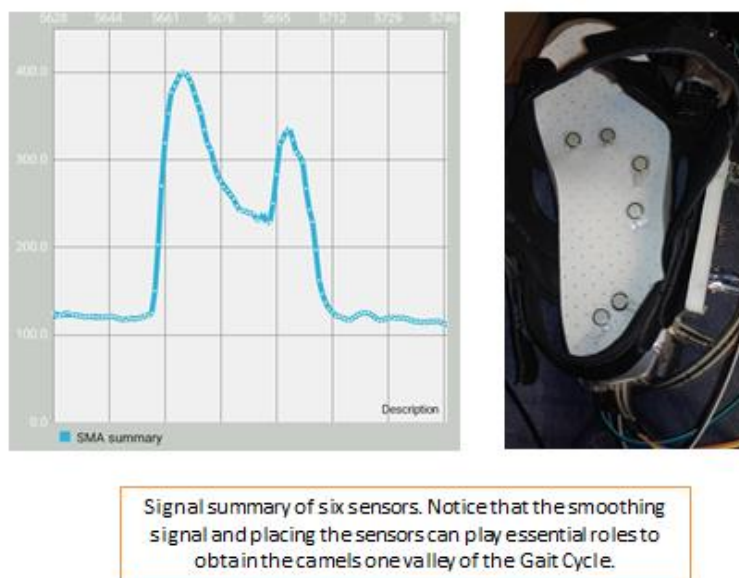
Figure 37 shows system circuit with a six sensors distributed at the heel, midfoot and metatarsal.

4.3. Peak Values and Time.

The data processing acquisition can achieve by either restoring the original information into local memory and then revoke the data to a PC for further analysis and pathological determinations. Like time to peak pressure, peak to peak, weight bearing, the center of pressure etc. Alternatively, the data can process immediately via serial port RS232 or Bluetooth connection during the run time and demonstrates the results [9]. However, in either cases, there are signal transmission errors that have to reprocess and filtered. In addition to the method applied in java Android (SMA with certain window size), the signal outcome (As mentioned in the previous discussion) went through downsampling/discard by N or every 1/N Hz in frequency. Down sampling works on reducing the effect of the sampling rate, and usually comes after converting the signal from analog to digital process A/D and low pass filter that works on anti-aliasing the signal, as shown in Figure 38.
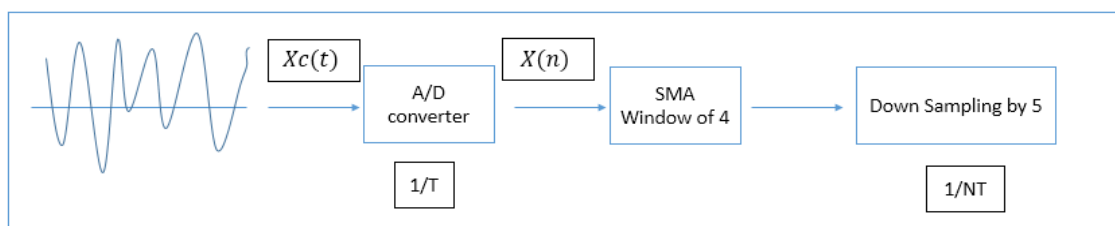
Figure 38 shows the system process on the pressure sensors signals from the foot.

Down sampling shows its effectiveness during the determination of the peaks. In addition, that the Android app is able to monitor the outcome graph in run time, it has the abilities to record the pressure data at the local internal memory *called myAppFile*. The app then can Recall

(Button) the data log to works on analyzing and down-sample in order to find the peaks, as the flowchart shown in Figure 39. The data algorithm followed in figure 39 is perpendicular slope base. It works as following:

It would first retrieve the data.txt file that has $1 \ X \ Multiple \ column. Say \ 1X4000$. After then there would be a for loop that starts from first value and take every five samples from vector to check the neighboring peaks (two adjacent values). The algorithm followed to check with a reference value. If the first value is less than 0, then set that value as a *value reference* with a *flag* (Alpha =1). I.e. the slope is positive. If the flag is equal one and the value reference is greater than zero, then that is the first peak (slope is now negative). This process will repeat over the data log until the end of file. The slope code written in MATLAB 2011.a. illustrated below.

Algorithm.1. Find peak values and time interval based on perpendicular slope.

- x=load('girl_1.txt');
- tmax= length(x);
- x4 = x(1:5:end);
- t1_n = 1:5:tmax;
- x1_n_ref=0;
- k=0;
- figure(1)
- grid
- plot (t1_n, x4,'b');
- hold on;
- for i=1: length(t1_n)
- if x4(i)>170
    - if x1_n_ref - x4(i)<0
        - x1_n_ref = x4(i);
        - alpha=1;

- o elseif alpha == 1 && x1_n_ref - x4(i) > 0
    - k=k+1;
    - peak(k) = x1_n_ref   ;
    - peak_time(k) = t1_n(i-1) ;
    - alpha = 2;
    - plot(t1_n(i),x1_n_ref,'r*','linewidth',1);

- o elseif alpha==2
    - x1_n_ref = x4(i);

- o end

- end

- end

x= load('girl2.txt')
tmax = length(x);
x4=x(1:5:end);
t1_n = 1:5:tmax;
x_ref = 0;
k=0;

For 1=1:;ength(t1_n)

If x4(i)>170

If x_ref - x4(i) < 0

Elseif Alpha==1 && x_ref - x4(i) > 0

x_ref = x4(i) ;
Alpha = 1;

K = K+1;
peak(k) = x_ref;
peak_time(k) = t1_n (i -1);
Alpha = 2;

Elseif Alpha ==2

x_ref = x4(i);
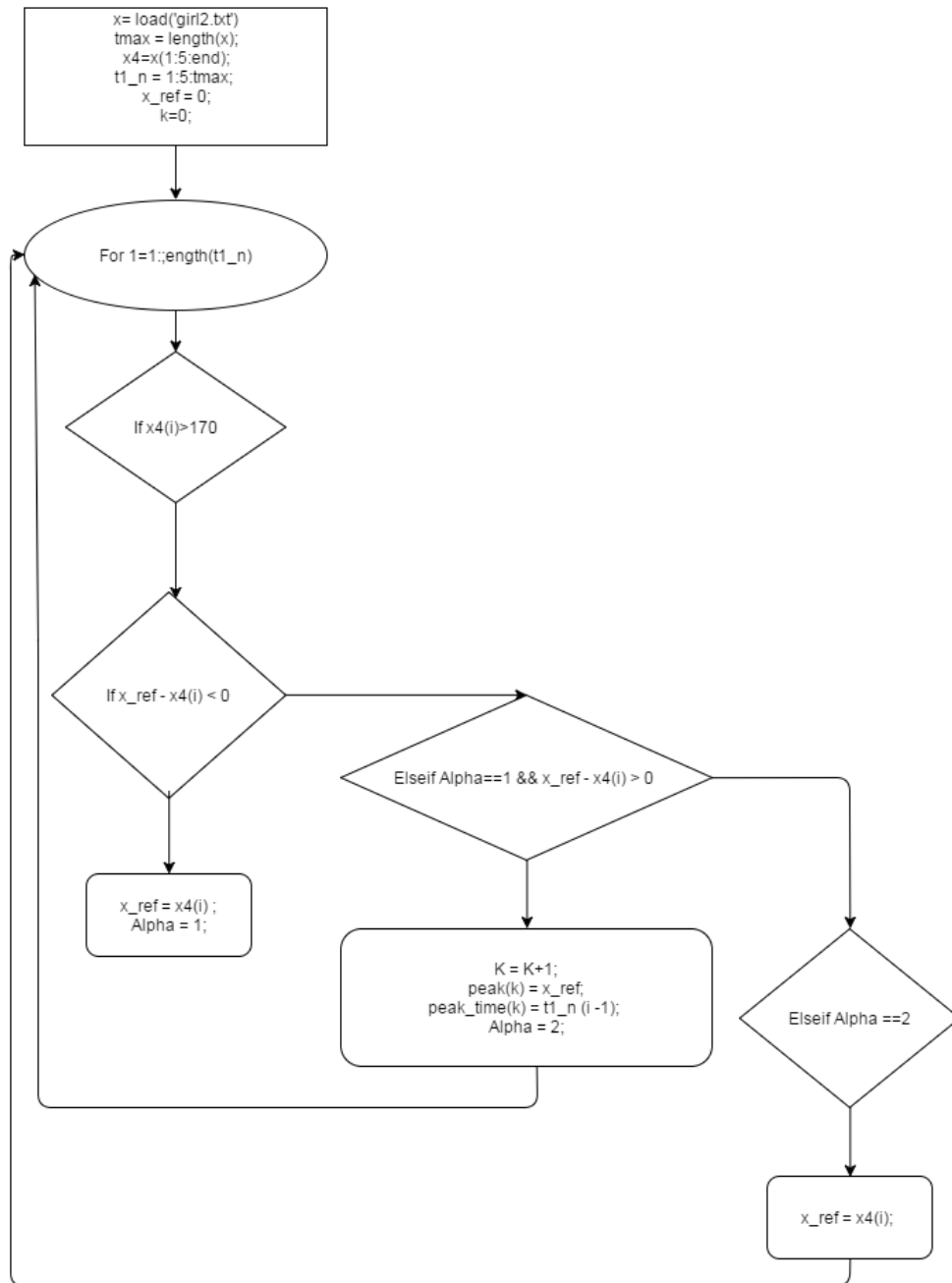
Figure 39.a illustrates the signal process to find the peaks in MATLAB in which it does the same through Recall Button in Android.

The function find peaks ( ) in MATLAB version 7.12. Signal processing toolbox did found the same peaks values applied at our trial data log. It tells nothing but the reliability of code applied and peaks obtained. Hence, find peaks have been adapted through its parameters to have the same results obtained in algorithm discussed beforehand, therefore, it can't apply as constant algorithm for other data logs, we were in need to an efficient algorithm in which it should work for the rest of walking patterns and can apply in Android java as well.

Findpeaks ( ) function MATLAB 2011.a. Shows the same results for peak values.

- D = load('girl_1.txt');

- Dmax = max(D);

- [pks,locs] = findpeaks(D, 'MinPeakHeight',Dmax/2, 'MinPeakDistance',20);

- figure (1)

- plot(D)

- hold on

- plot(locs, pks, '*r')

- hold off

- grid
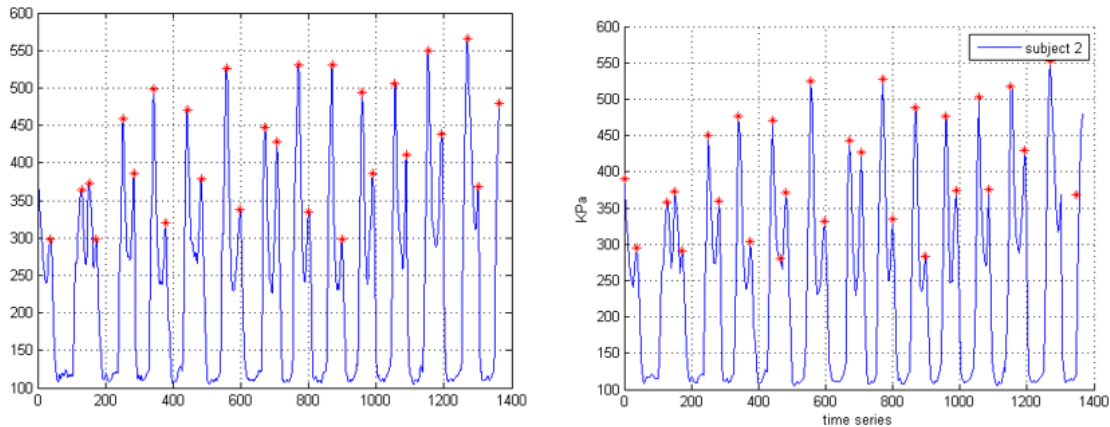
  Figure 39.b shows the peak values and time series obtained in find peaks function and slope base

The figure shows that the function has the same peak results in slope base. Where the left graph is for find peaks ( ) function, and right graph is for the slope perpendicular.

We have chosen to sample by five to skip the unwanted peak that may occur during the process of the slope. The graph result of the peak values using downsampling shown in Figure 40 and compared with the original values. Simplest reason for downsampling is to reduce the amount of data we have. It would reduce the data rate to let the perpendicular slope finds the peaks smoothly, and to mitigate aliasing distortion.
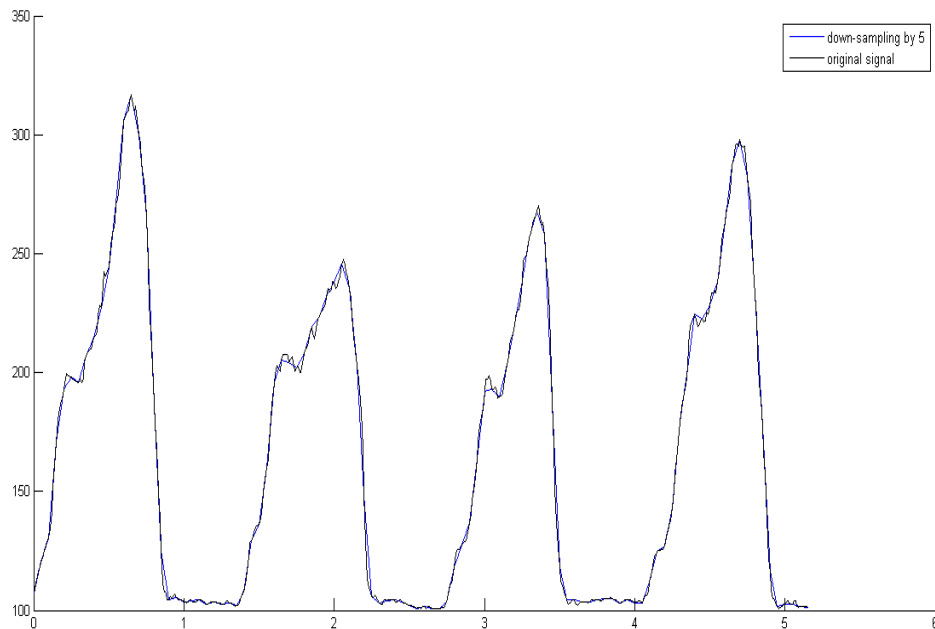
Figure 40 shows the MATLAB 2011.a. downsampling effects compared by original signal.

In figure 40, it shows a demonstration of a male subject walking pattern for nearly 5 seconds (516 samples). The logic applied found eight pure peaks with the time interval of each peak.

Peak values in KPa.	Peak time in sec.
198.1520	0.250 (time to peak)
316.9850	0.6500
205.2155	1.6500
245.5190	2.050
192.7505	3.050
267.9560	3.350
224.7440	4.40
297.8720	4.70

Peak-to-Peak time stands for the phase time. It can determine if a one subtract the second peak from the first peak and divide by 100 from the first column. Alternatively, the peak-to-peak time interval of each step can obviously determine from the second column of the table above.
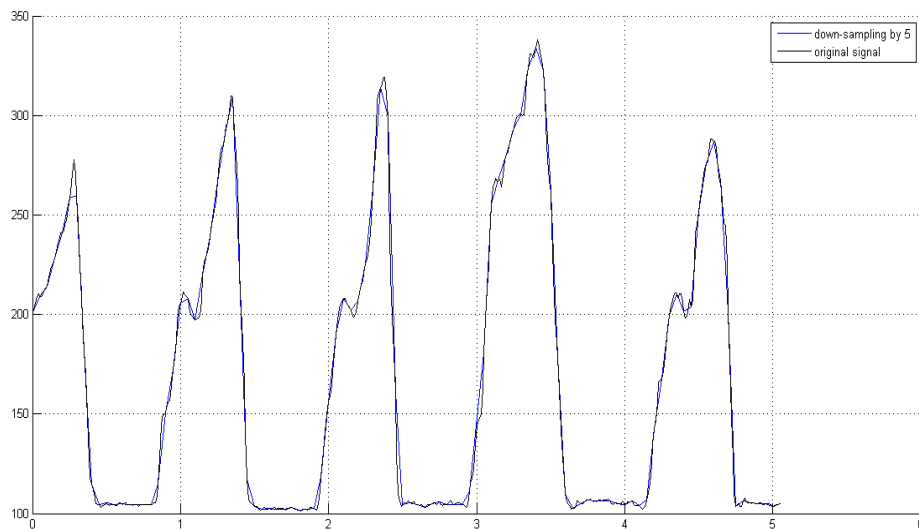
Figure 41 shows the second trail walking pattern recorded from Android and recalled by Matlab to determine the peaks.

Eight peaks found from 5 seconds walking normally at average 2 feet each step.

Peak values in KPa.	Peak time in sec.
259.2305	0.3000(time to peak)
208.1240	1.0500
309.5060	1.3500
208.1240	2.1000
314.0765	2.3500
334.4360	3.4000
210.6170	4.350
286.6535	4.60

From figure 40, 41 and their peaks timetables. It is clear that there is a periodic signal between each peak with its neighbor. The first trail from figure 40 shows that there is a periodic peak every 0.4 second. The second trial from figure 41 and the table shows that there is a periodic signal at almost every 0.3 seconds. However, a one can drop the unshaped signal as it does not have two peaks, therefore, a one can take the next phase of the step. Parameters extracted let us extend the study to introduce the mythology explained by Che-Chang Yang et al [24]. Yang demonstrated the tri-axial accelerometer without the use of sensors. The accelerometer used in human detection classification. It can provide parameters about ambulation, rehabilitation, fall detection, cadence, step length, stride regularity and trunk acceleration by using autocorrelation process.

The autocorrelation is one way of recognition method. It is based on estimating the repeated characteristics over a signal sequence periodic phase. Considering a series of array with N points $[x_1, x_2, x_3, \ldots]$. With a given phase shift (m), the unbiased autocorrelation would be:

$A_m = \frac{1}{N-|m|} \sum_{i=1}^{N-|m|} x_i \, x_{i+m}$. In figure 42 is an example of autocorrelation results from vertical acceleration of the body (VT) and antero-posterior (AP). Where the wearable accelerometer raped at the waist of the subjects during the normal walking. The first phase shift called zero phase in which it stands for the first period, while D1 stands for the second phase and so on.
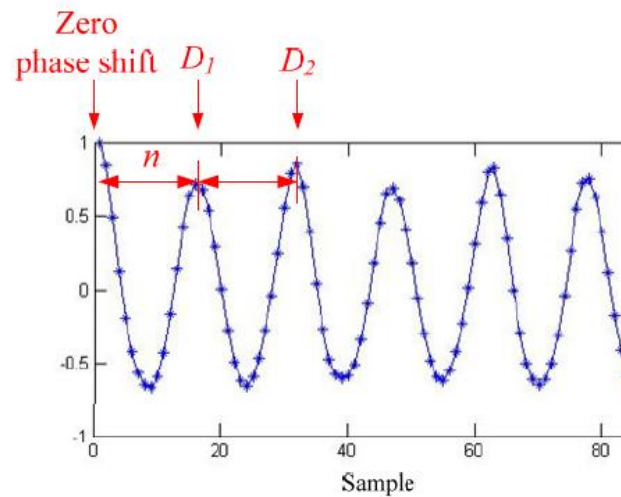
Figure 42. An example of autocorrelation from a vertical acceleration at the waist of the body's subject [24].

D1 and D2 represent the step and stride regulatory respectively with m-point considered as the duration of one-step.

Yang was able to determine each of cadence and step symmetry for walking classification from healthy and PD patient (Parkinson's disease) subjects [24]. By comparing the cadence between the two groups and gait regularity average. It concluded that PD patients weren't able to have the repeatability of steps and strides compared with the healthy subjects, Yang compared the results using the video capture system in which it uses for the same analysis purposes. Statistical analysis including ANOVA test was involved in the study. As shown in the table below.

	Multiple sliding windows			Entire single window
	Mean coefficient of variance (CV)	Mean percentage error	Mean ± SD	
Cadence (steps/min)	1.21%	0.67%	113.3 ± 4.1	111.1
			103.4 ± 0.0	103.4
			111.1 ± 0.0	111.1
Step regularity	8.53%	2.44%	0.763 ± 0.073	0.793
			0.679 ± 0.042	0.665
			0.785 ± 0.077	0.773
Stride regularity	9.34%	4.47%	0.869 ± 0.128	0.903
			0.793 ± 0.052	0.746
			0.816 ± 0.061	0.877
Step symmetry	7.78%	2.04%	0.884 ± 0.061	0.878
			0.858 ± 0.057	0.892
			0.867 ± 0.085	0.881

Table 5. shows the statistical analysis obtained from Yang [24] studies.

Research and literature review utilized the research study parameters – like peak times and peak to peak - in comparing their system with other commonly used system like Pedar in-shoe system from Novel GmbH Germany. The initial results can compare between healthy and unhealthy subjects that have the same spatial parameters (speed, cadence, steps, time, age, and weight). Also, other studies aspects had focused on placing the sensors as a matrix measurement to have as many parameters as it can from the foot during the GC, or placing the sensors as a discrete measurement using sensors placed at a certain position. For instance, Marcelo P. de Castro et al [25], designed a monitoring system and called it WalkinSense. Marcelo tried to measure Pressure peak, pressure peak time, and pressure-time integral and mean pressure in eight different regions in the foot. These parameters compared with Pedar German system in a dynamic experience process in terms of accuracy and repeatability results. The data collected from the system used a micro-electromechanical system MEMES accelerometer, one

gyroscope connected with the eight-piezo resistors with sampling rate similar to the system research (100Hz), and with two different mode operation. Offline to record, the data in local memory and on runtime to send the data over Bluetooth technology to a PC. Subjects asked to walk 100 steps per minute and by the time, 12 steps recorded for statistical analysis in MATLAB 7.0 figure 43.

(a)   (b)
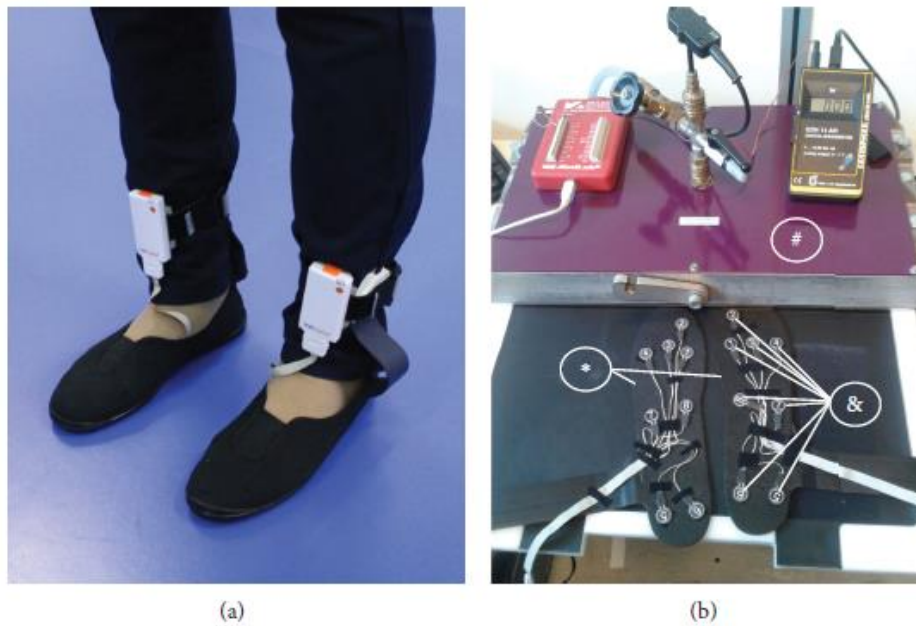
Figure 43 shows WalkinSense and Pedar system attached, and sensor placement at the eight regions of the WalkinSense system.

Four parameters were determined in this study and compared with Pedar system to determine the repeatability and accuracy. The parameters found in Marcelo study are -

1. The Peak Pressure in KPa and defined as the maximum value displayed with respect to the stance phase.

2. The Peak pressure time of the stance phase,

3. The mean pressure and defined as the pressure processed during the stance phase,

4. The pressure time integral in KPa.

4.4 Data analysis.

Usually, data analysis can be observed in likewise studies used to classify the movement patterns. In which it uses the pressure sensor underneath the floor or the in-shoe with attached circuit to classify the GRF as an example. However, there are varieties of pattern classifications can be used like template matching, statistical classification, and neural network. For example, Microsoft EasyLiving group mentioned by Robert and Rupert [26] used a pressure sensor on the seat cushions to identify if the subject is sitting or standing, as one way of nonverbal communication similar to gesture recognition. Robert and Rupert classified four different motions: step, crouch, jump-drop land, and finally rise to stand and sit by using HMM (Hidden Markov Model). Samuel Pfaffen et al [27] has developed an app called Planipes that communicates with 16 FSRs. The circuit regulations used two multiplexers (2 outputs) to regulate each two sensors at a time, with the use of Atmel ATmega328 microcontroller 8-bit ADC 40 Hz. The microcontroller samples the voltage of all 16 sensors in a round-robin scheme. This type of study didn't analyze the data log collected, although it uses the same methodology in our study. Also, Samuel used GPS service from a mobile to monitor the steps of each foot, but studies have shown that GPS is not suitable to be used indoors and can't give precise readings as our study has proven.

However, in addition to the aforementioned studies from what we have performed from experimental trials of placing the sensors, sampling and analyzing in order to find peak values, A further analysis was done by using correlation coefficient methods on two different walking patterns for one subject and between two different subjects.

Normal walking and fast walking are tested for one subject (26 age, 173cm, 70.5kg), and for a distance (d) equal 16.2 meters.

	Normal walking	Fast walking
No. of steps taken	25	20
Cadence (steps/sec.)	1.561	1.935
Time taken in seconds	16.01	10.335
Av. Velocity (m/sec).	1.0306	1.567
Av. Gait Cycle	1.2808	1.0355
Av. Step length (m/setp)	0.648	0.81

Table 6 show the two-sample process from two different walking pattern for one subject.

Three Flexi-Force sensors - attached with the circuit attached to the sandal – are placed at the heel, 1st metatarsal, and 5th metatarsal. The goal of data analysis is to tell and extract some features between the two patterns. 600 samples were plotted to demonstrate the data and peaks in which it showed in figure 44.a and figure 44.b, a one can notice the foot clearance and stance phase.
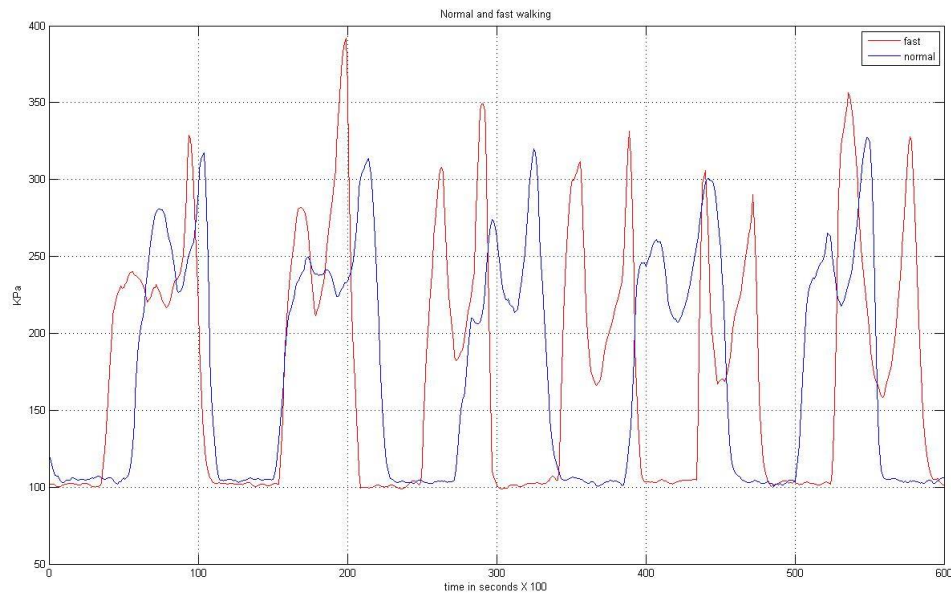
Figure 44.a shows the walking patterns generated from one subject and sampled by 100 samples per second.
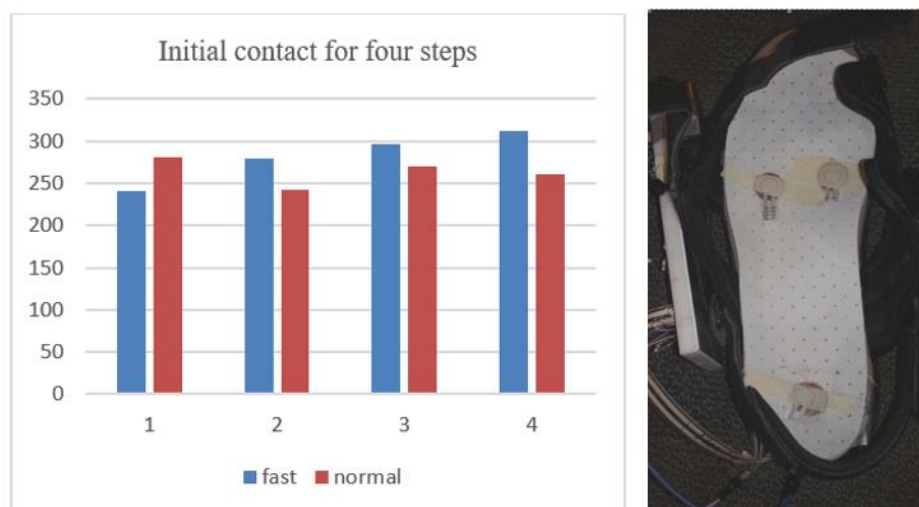
Figure 44.b shows classification between initial contacts - first peaks given for four steps.

We have chosen to haven three sensors because of the analysis of the significance of the pressure sensors data has shown that sensors at the heel and 1st metatarsal head have the most significant predictive power.

4.4.1 Correlation Coefficient

In this experiment, a correlation coefficient used to measure the linearity/strength of the associated variables between the two processes (normal and fast walk). Correlation coefficient or so-called Pearson product moment correlation coefficient is denoted by (r), where the value outcome is always between -1 and 1. In which it is positive if the variable gets to be bigger, and the second variable process is getting bigger, while (r) is negative when one process gets bigger in values, and the second process gets decreases. The experimental results of this study show weakness linearity between normal walk and fast walk with equal size of arrays (900 samples). That is close to zero, r=0.249

$$r = \frac{\sum xy - \frac{\sum x \sum y}{N}}{\sqrt{\sum \left\{ x^2 - \frac{x^2}{N} \right\} \{ \sum y^2 - \frac{(\sum y)^2}{N} \}}}$$

2-D Correlation coefficient

- clear all;

- normal_w = load('normal_w.txt');

- fast_w = load('fast_w.txt');

- nor_walk = normal_w (1:900);

85

- fst_walk = fast_w (1:900);

- r_cpr = corr2(nor_walk, fst_walk);

r_cpr =0.249

4.4.2 Cross Correlation

Cross correlation is a measure the similarities between two signals at different time lag positions. I.e. It is whether two signals matched or not. The Lag correlation explain the sequence of two-time series shifted in time with respect to the second one. One of the process may have delay rather than another. By defining the cross-covariance function, and considering N is the number of pairs of observation at time x, and y.

$$C_{xy}(k) = \frac{1}{N} \sum_{i=1}^{N-k} (x_i - mean\ of\ x)(y_{i+k} - mean\ of\ y) \dots [k = 0,1,2,3, \dots, (N-1)]$$

$$C_{xy}(k) = \frac{1}{N} \sum_{i=1-k}^{N} (x_i - mean\ of\ x)(y_{i+k} - mean\ of\ y). [k = -1,-2,-3,\dots,-(N-1)]$$

$$r_{xy}(k) = \frac{C_{xy}(k)}{sqrt((C_{xx}(0)C_{yy}(0))}$$

Where Cxx (0) and Cyy (0) are the variances of x and y.

The cross-correlation shown in figure 45 shows aligning vertical between the two process patterns (normal, and fast walking) to maintain the correlation. At the lag =11, between the two variables, shows strong correlation/similarities between the two processes.   When one of the

signals shifted from another, a one can see a correlation measure at lag from 400 to 600 (weakness sequence correlation).
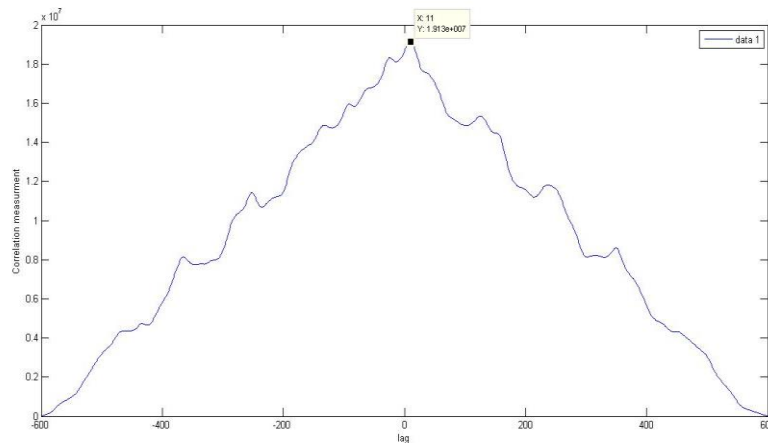
Figure 45 shows the cross-correlation measurements taken from the normal and fast walking.

In fact, the two walking patterns do not have the same length, therefore, and by using MATLAB R2011. a. the two processes were set to have samples from 1 to 600, and then executes the cross-correlation to return the lag.

Find Cross Correlation.

- normal_w = load('normal_w.txt');

- fast_w = load('fast_w.txt');

- nor_ = normal_w (1:600);

- fst_ = fast_w (1:600);

- [corr_seq lags] = xcorr (nor_, fst_);

- figure (2);

- plot (lags, corr_seq);

- xlabel('lag');

- ylabel ('Correlation measurement');

The statistical analysis may use in foot deformity. Sicco A. et al [28] discussed the therapeutic footwear in ulceration and diabetic. In which the goal is to reduce the peak pressure at the Region of Interest (ROI) in five types of footwear modifications. By using Novel Multi-mask software, masks were drawn for the heel, medial, and lateral midfoot, 1st metatarsal, second and third. The peak pressure and pressure time integral (Peak to peak time) were calculated using ANOVA and t-test in SPSS. The results showed there was no difference in mean peak pressure obtained from the ROI that is placed in different foot areas (Optimization), and the study was considered as one way of significant pressure relief.

4.5 Normal and Slow Walking

For a further analysis in which it used the same approaches of cross-correlation and coefficient, one subject (26 age, 171kg, 173cm) asked to walk the same distance previously mentioned in two different walking pattern (slow walk, and normal walk). Where a number of steps taken, time and speed illustrated in the table below. However, the table may tell nothing about the induvial step characteristics unless either distinguishes visually by analyzing the signal base on peak values and time interval for each as mention before in 4.3.

Distance 16.2 m.	Slow walking	Normal walking
No. Of steps	32	23
Time in seconds	26.772	16.948
Cadence (Step/Sec)	1.195	1.357
Velocity (m/sec)	0.605	0.955
Step length (m/step)	0.506	0.704
Average Gait cycle	1.673	1.473

Table 7 shows basic spatial parameters between slow and normal walking.

Six hundred points were (for 6 seconds) chosen to plot for both normal and slow patterns. Where the coefficient is taken for a fixed one-step (break down to nearly 2 seconds) was -0.1154. While the cross-correlation for the one-step in shown in figure 46 and 47.
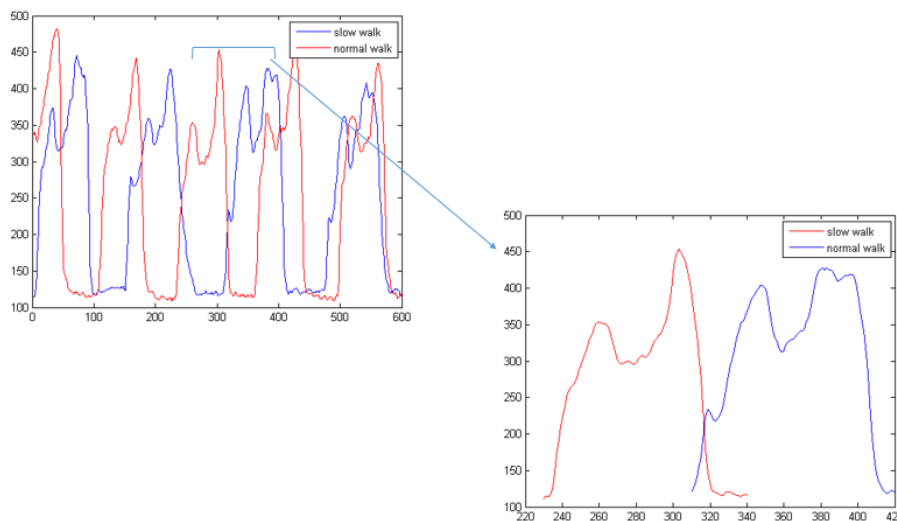
Figure 46 shows the signal steps for 6 seconds and one-step chosen for correlation test
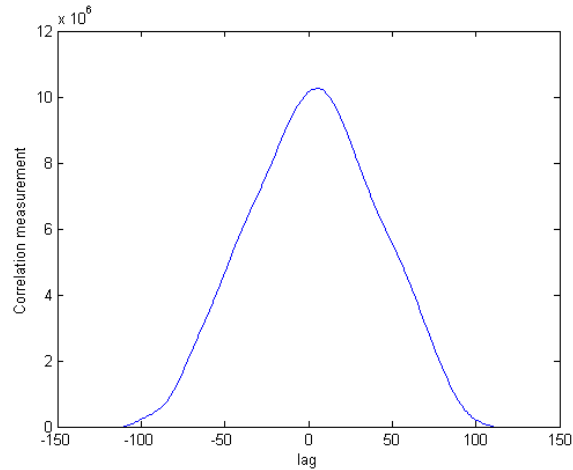
Figure 47 shows the cross-correlation for one-step taken between normal and slow walking for 110 points.

From figure 46, it is obviously clear that normal walk for six seconds with same distance taken - regardless the slow walking - is not the same as if the subject walked slowly for the case of illness or injury. Consider the case if a one take a frame of four steps (a frame of 6 seconds) from slow and normal data logs, and break down each step aside for classification purposes as shown in the table below.

normal_w mean	normal_w maxima	slow_w mean	slow_w maxima
248.8825	441.635	285.1819	445.1667
256.4594	453.8922	281.8787	426.4693
261.8969	454.1	294.6253	427.9235
258.5454	435.1947	275.4058	408.395

A one can notice that the there is no overlapped between the means of normal_w mean and slow_w mean. The same analysis for local maxima of each step taken along with the means are

demonstrated in figure 48.a and 48.b shows the results between slow and normal walk for the same subject.
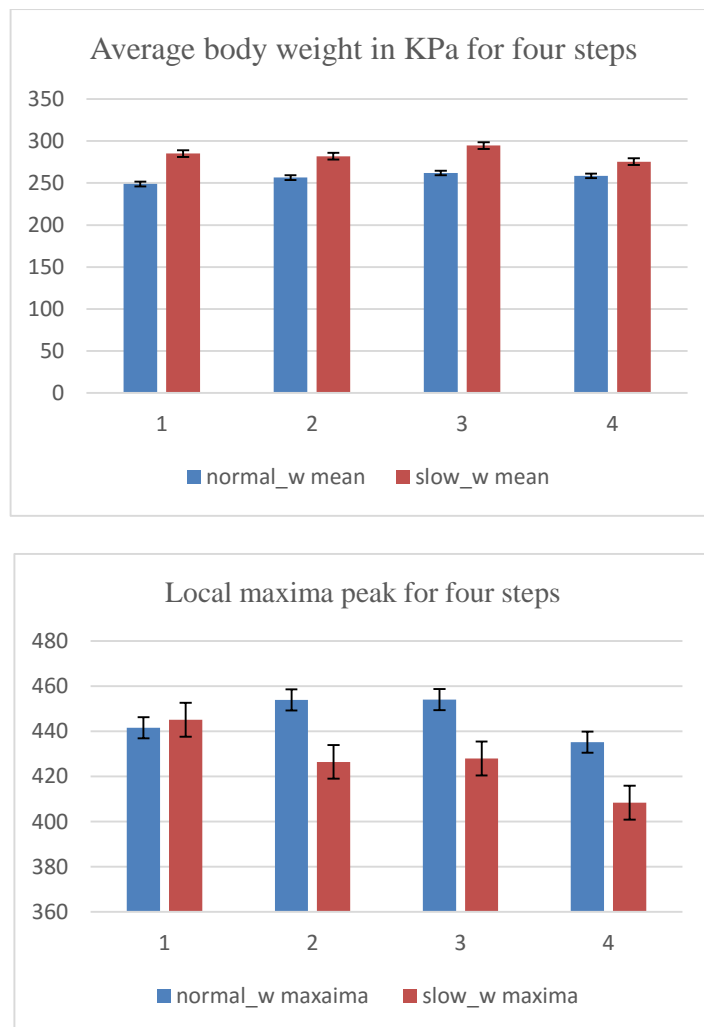
Figure 48.a shows the local maxima peak values, for both slow normal and average body weight for four steps.
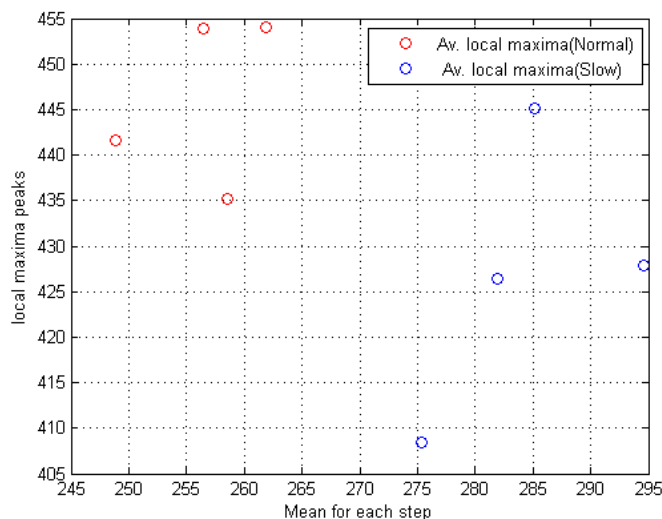
Figure 48.b shows the scatter points from one subject at slow and normal walk patterns.

Although this experiment was done at an individual time between normal and slow trials, in pathological gait, when pathology affects one foot rather than other, the body will try to spend a shorter time on the "injured" foot and regardlessly, the longer on the good one (Same as Antalgic gait). Shorting the injured foot tells bringing the healthy one to the ground as soon as possible. Therefore, it is shorting both the time duration of the swing phase and the step length. That can conclude, a short step length on one side means issues with single support on the other side.

4.6 Comparison between female subjects

Two healthy female subjects - within average age 22 –asked to walk on a floor with 16.2 meters. Both subjects practiced wearing the sandal system for a certain distance before starting the trials. Three Flexi-Force sensors were affixed in-shoe at the left foot with the circuit attached. Subjects average weight, speed, and cadence provided in the figure below. We considered timer

provided within the app features. However, the accuracy of time taken for both subjects while walking could find in figure 50 (Sampled 100 samples/second).

	female_1	female_2
# steps	27	19
time in seconds	15.252	9.108
av. weight	130lb	112lb
tall	5.5	5.5
cadence step/sec.	1.77	2.086
velocity m/sec	1.063	1.778
step length m/step	0.6	0.852
av. Gait cycle	1.13	0.958
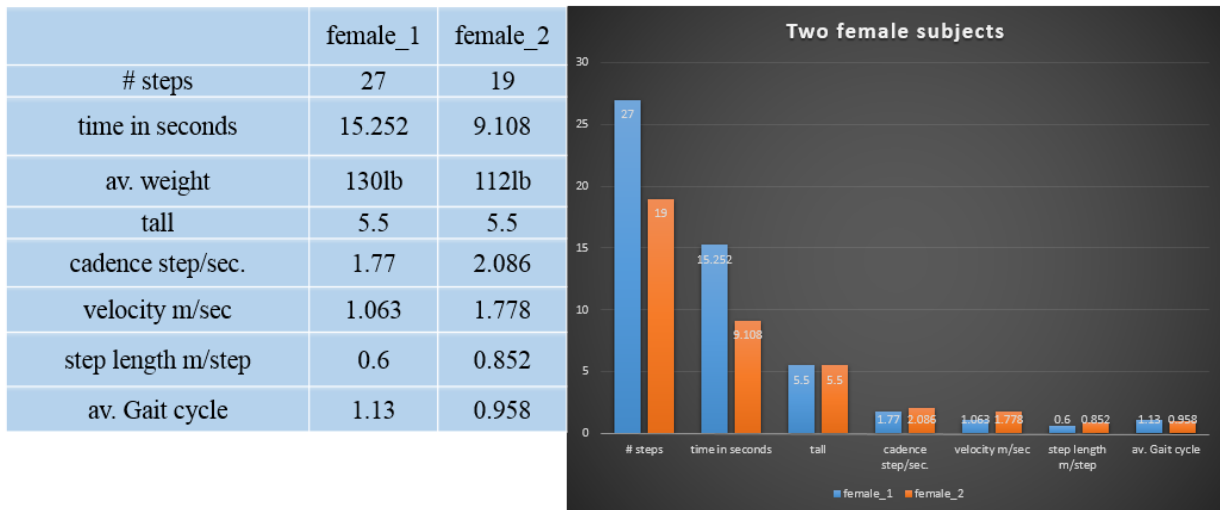
Figure 49 shows two females spatial parameters.

The original data log of both subjects collected from the app demonstrated in figure 50. A one can notice several features can extract especially time series and peak values. The subject 2 with a blue line signal has a long swing periodicity regardless to subject one with a red signal. I.e. The foot clearance of the floor.

As far as ground reaction force is concerned, the task of weight acceptance and start of stance and swing for subject 2 (blue signal) are classified into two phases. Initial contact and loading response. Within the IC, the start stance with heel rocker occurs with respect to the impact declaration, while in Loading response, the clearance occurs in shock absorption with weight-bearing stability. Notice that the demonstrated data are already downsampled by 5, with a simple moving average window size 4 at Android side. The peak pressures generated from both

subjects for 800 samples (8 seconds) also classified based on peak value and time and they demonstrated below.
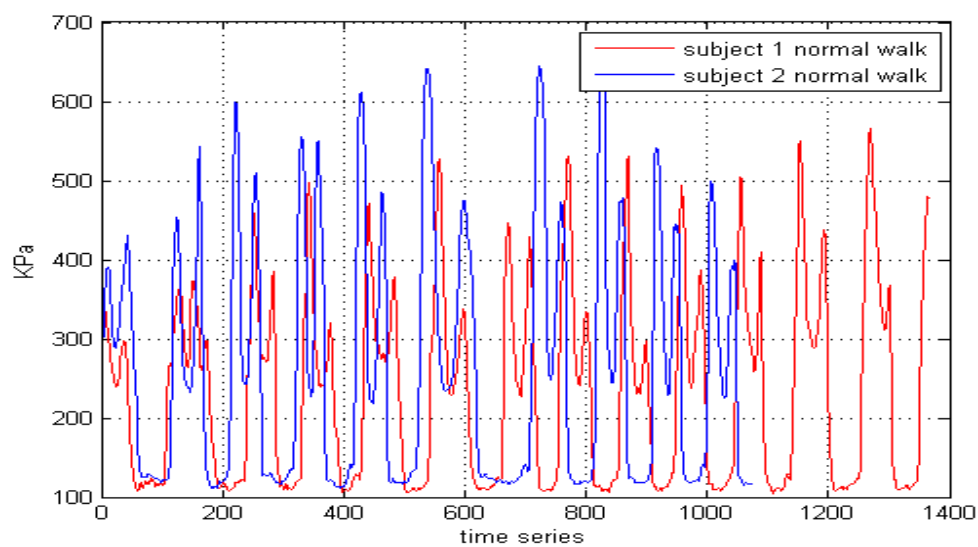
Figure 50 show the data log of both subjects
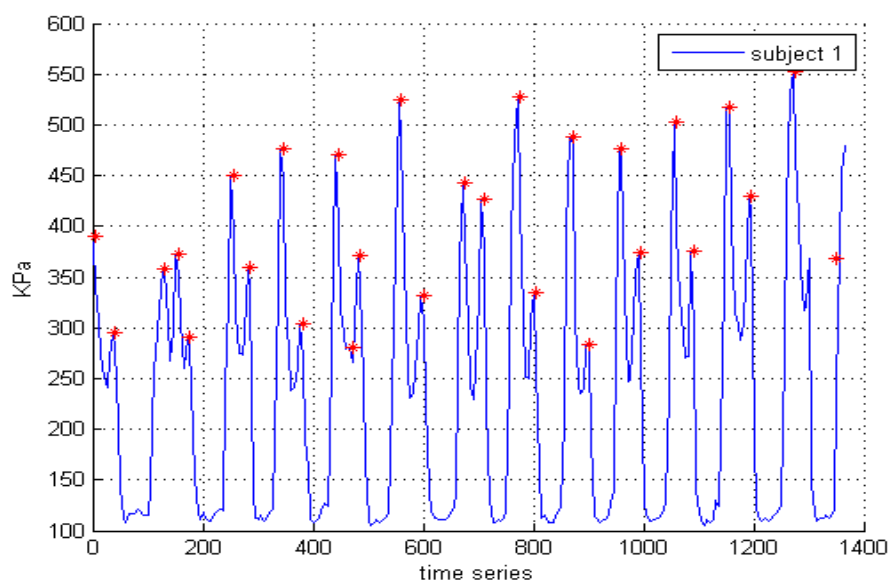
Figure 50.a shows normal walk original data for subject 1.
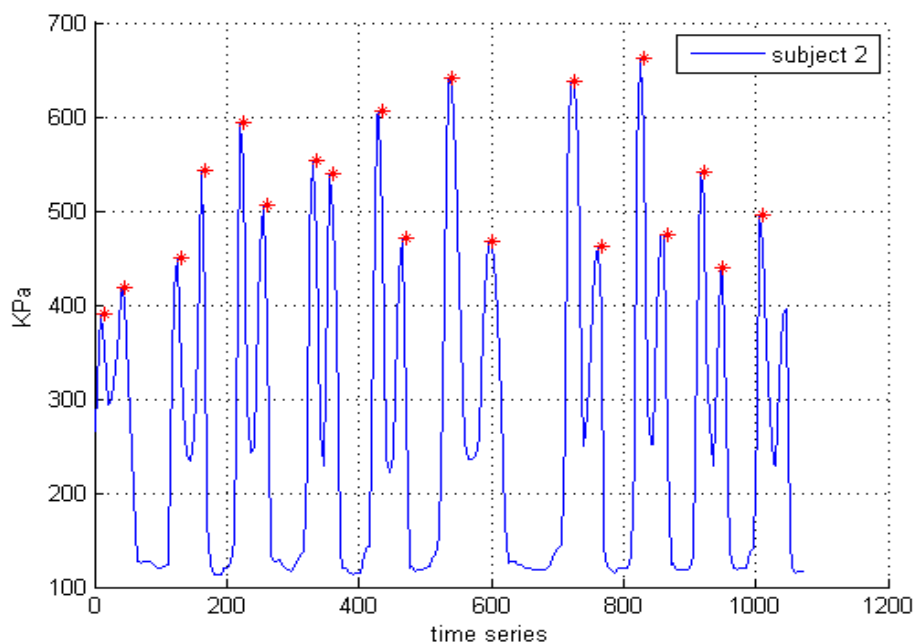
Figure 50.b shows normal walk original data for subject 2.
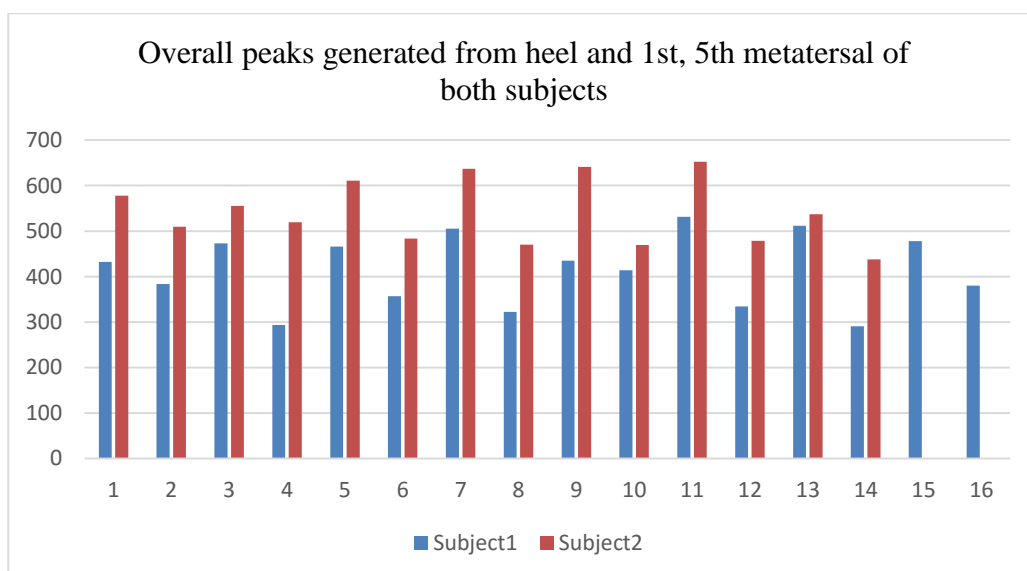
Figure 51.a shows the peak values from the foot contact at the center of the heel and 1st, 5th

metatarsals – for 800 samples picked from data log of both subjects
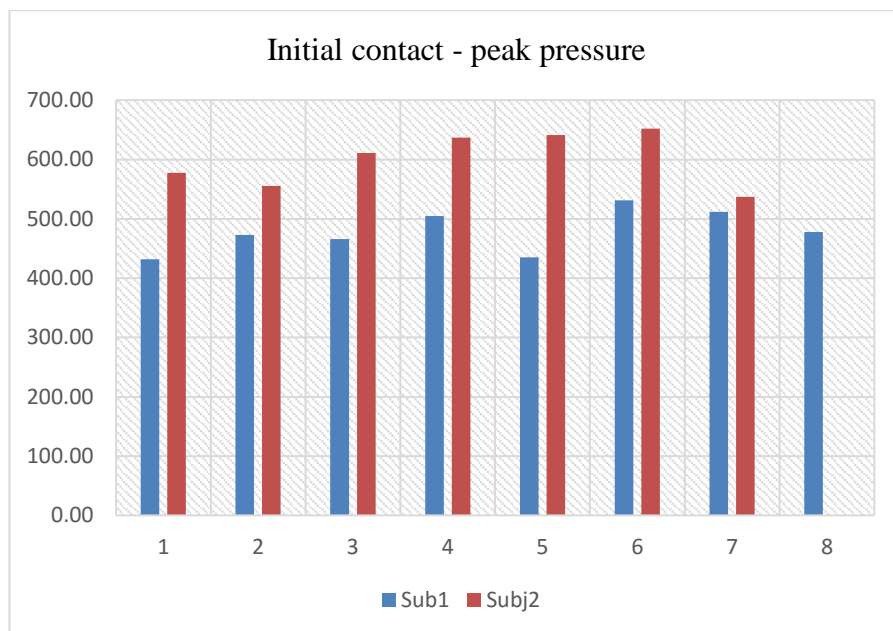
Figure 51.b shows the peak pressure at the initial contact
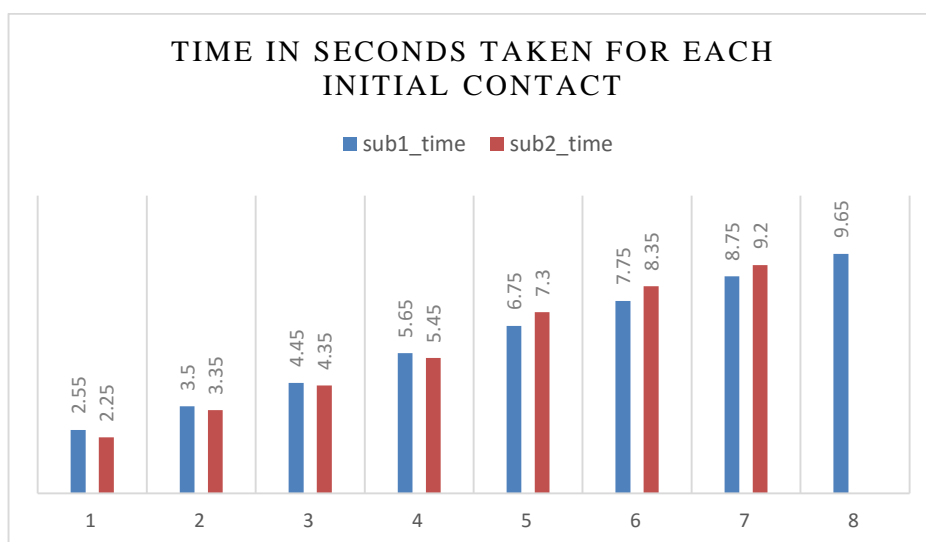
Figure 51.c time series of each initial pressure contact in figure 51.b

Although the following test scenario done between two healthy subjects, but it may add to pathological patterns arguments. Now to questioned if the peak plantar pressure is useful to indicate the state of disease and its further consequences, a hypothesis test performed between peak pressures of both subjects to see if there is a significance difference between their GRF generated with respect to their walk pattern. Hence, the number of peaks generated from two subjects were less than 30 samples (population), and their samples are independent on each other, therefore we picked two-sample hypothesis test unequal variance. If we assume that null hypothesis is the assumption as there is no difference between the initial contact peaks – and the alternative hypothesis is as there is the difference in peak pressure at IC between two subjects. As shown in table 8 demonstrated below that the T-test for $two\ tail\ P(T <= t)\ two-tail$ is much smaller than alpha (95%. The significance level). We will reject the null hypothesis that claimed there is no differences between peak pressures. We have enough evidence support our claim for the alternative hypothesis that says there is significance difference between the peak pressures for the two subjects.

$\alpha = 0.05$

$$H\theta: \mu = 0. There\ is\ no\ difference\ in\ peak\ pressures.$$

$$H1: \mu \neq 0. There\ is\ difference\ in\ peak\ pressures.$$

$$P\ value < \alpha. will\ reject\ the\ null\ hypothesis.$$

t-Test: Two-Sample Assuming Unequal Variances		
	subj_ 1	*Subj_2*
Mean	478.9256863	601.7212
Variance	1264.183868	2054.416
Observations	8	7
Hypothesized Mean Difference	0	
Df	11	
t Stat	-5.778942368	
P(T<=t) one-tail	6.1514E-05	
t Critical one-tail	1.795884819	
P(T<=t) two-tail	0.000123028	
t Critical two-tail	2.20098516	

Table 8 shows the hypothesis test for peak pressure at the IC – data obtained from

Figure 51.b.

The peak-to-peak time taken for each subject illustrated in figure 51.d. Although peak-to-peak time is between 0.3 to 0.35 seconds, but their major difference was in cadence and velocity. Such major difference (demonstrated in figure 49) may result from related small or big differences in knee flexion during weight acceptance and midstance. That may reflect the drastically increase in vertical acceleration of the body, as the cadence increase [31].
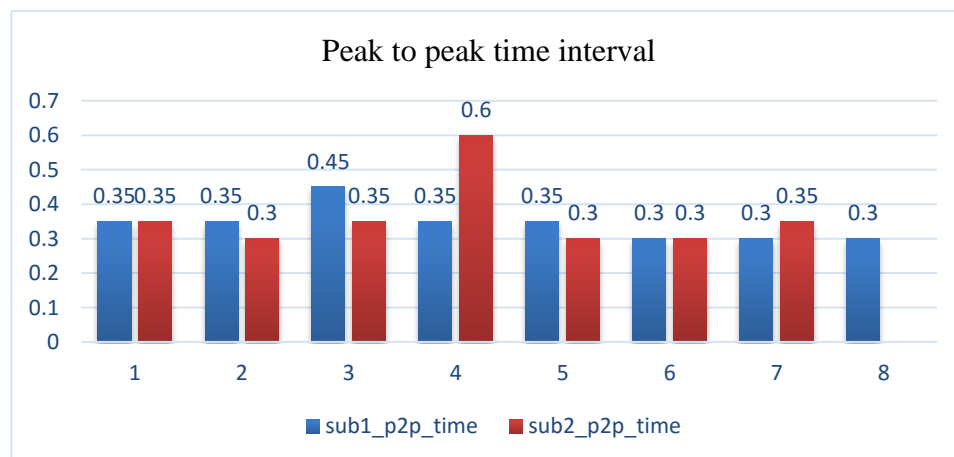
Figure 51.d. shows peak-to-peak time interval for the two subjects.

4.7 Partial foot bearing using binary logistic regression

Logistic regression is one of the methods that belongs to Generalised Linear Model (GLM), and it is an alternative to Fisher classification. It is commonly used for marketing, finance, and clinical studies. Logistic regression can classify between healthy and unhealthy walking pattern as one application.

Logistic regression assumed that we have a series of N observed data points. Each data point v consists of a set of k explanatory variables $x_{1,i}$ ... $x_{m,i}$ (also called predictor variables, input variables), and an associated binary outcome variable Y_i (also known as a dependent variable, response variable, output variable). The goal of logistic regression is to explain the relationship between the explanatory variables and the outcome. So that an outcome can be predicted for a new set of explanatory variables. The explanatory variables may be any type of real-valued, binary, categorical. While the dummy variables (dependent variable) are taking the value of 0 and 1, in which they assigned for each possible of the discrete variable. A simple example of a discrete variable is the blood type. It has four possible values. A,B,AB,and O. They can assign to four separate regression coefficient to be matched for each possible value. Therefore, the four separate values would convert into two dummy variables as the following. "is-A, is-B,is-AB,is-O". Where only one of them would be 1 and the rest are 0. That would follow the Bernoulli-distribution method (probability of success). Logistic regression (LR) is developed from odds ratios and probabilities.

The odds ratio is used to measure the association as it estimates how much likely/unlikely the outcome to be present the probability variable is close to 1 or 0.

 The probability using Logistic regression is always between 0 and 1. That means the dependent variable in logistic regression follows the Bernoulli distribution that is having an unknown probability p (prob of success) and 1-p (prob of failure). LR is the estimation of an unknown p for any given linear combination of the independent variables. To link the independent variables to the Bernoulli distribution, that is what we call it Logit.

$$\ln(odds) - - \rightarrow \ln\left(\frac{p}{1-p}\right) that\ is\ the\ logit(p).$$

The range is from negative infinity to positive infinity.

The inverse of the Logit – where the p is between 0 and 1. Assumed that $\propto$ *is some number*

$$logit^{-1}(\propto) = \frac{e^{\propto}}{1+e^{\propto}} = \frac{e^{\propto}}{1+e^{\propto}}$$

Where in our case the some number is the linear combination of variables and their coefficients

The inverse –logit will return the probability of being "1" or in the event of occurs group.
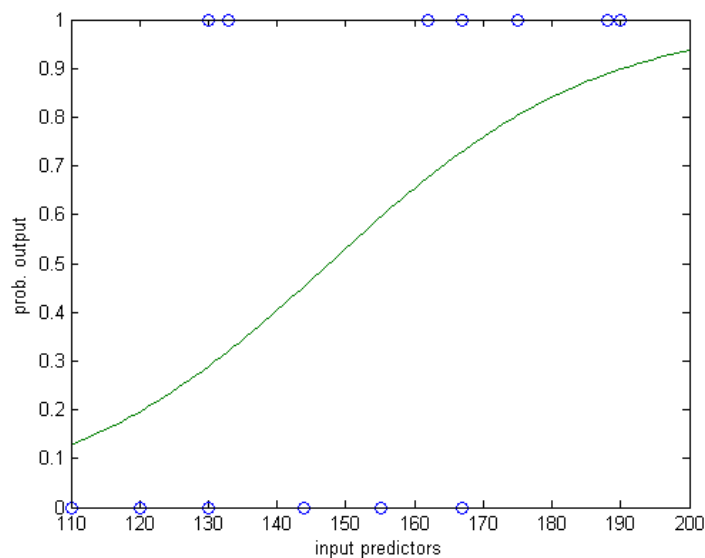
Figure 52 shows the logits regression curve for the estimated model.

The natural logarithm of the odds ratio is equivalent to a linear function of the independent variables. The antilog of the logit function allows us to find the estimated regression equation. We sufficiently give the final equation for p estimated without going deeply to the linear algebra.

$$logit(p) = \frac{p}{1-p} = Bo + B1X1. \, Solving \, for \, p \, would \, give \, us$$

$$\rho = \frac{e^{\beta 0 + \beta 1 x 1}}{1 + e^{\beta 0 + \beta 1 x 1}}$$

p is between 0 and 1. βo Controls the location of the midpoint, $\beta 1$ control the slope. $x1$ is the predictors

There are a lot of extensive papers and tutorials about how to plug in the coefficients to find the estimated p and the odds values [29][30]. The advantages of logistic regression are:

1- No assumption for classes in feature space.

2- Good accuracy.

3- Dimension space can be continuous, categorical or binary.

However, when a patient can't put his/her full/normal load into one leg, it is called partial foot bearing. Partial foot bearing is used after procedures to achieve gradual recovery and limit the percentage body weight. Subjects were asked to perform weight bearing as there is a knee flexion problem using one crutch at the side of the problem leg. The same subjects, however, were asked to perform walking by their normal full load using the wearable shoe sensors.

Data has been collected from 12 subjects (Age 25±3.9, Weight 167±24, Height 5.6±0.33); all subjects signed the Institutional Review Board consent form. Each subject practiced walking using the crutch for more than 10 meters to assure repeatability and utilize the data obtained

from each subject. The results of their average full load were ~229.2 KPa with STD 40.6 while their partial foot bearing were ~167.93KPa with STD 28.3. The differences between their full load and partial weight bearing were considered 39% of the Body Weight (BW). The peak to peak time interval in the normal walk was ~0.34 secs with STD 0.05 while the partial foot bearing was 0.22 secs with STD 0.086. Logistic regression is used to distinguish between their peak pressure during the full load and partial foot bearing. The original dataset of their average peak pressures is demonstrated in figure 53. Assumed subjects who performed full load took the value of 1 while the same subjects who performed partial weight bearing took the value of 0. The dataset used in this study is demonstrated in figure 53 .
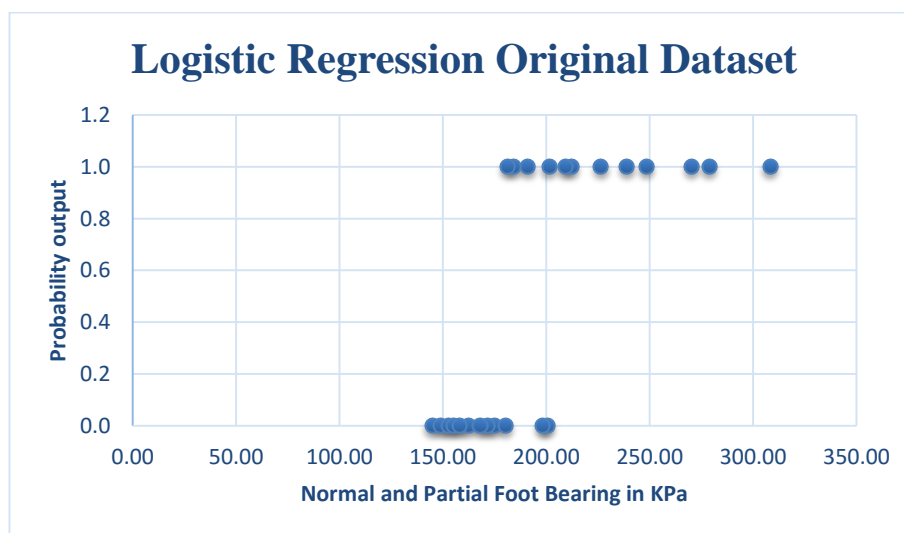
Figure 53 shows the dataset between full load and partial foot bearing.

By applying logistic regression using Excel, the trained data results showed the correctness of each dataset with the final accuracy equalling 82.6%. The coefficients model for logistic regression is:

$$p = \frac{e^{-19.6+0.11x}}{1 + e^{-19.6+0.11x}}$$

Figure 54 shows the extracted peak pressures from subjects who performed full and partial weight bearing.

Logistic Regression										
201.40	Success	Failure	Total	p-Obs	p-Pred	Suc-Pred	Fail-Pred	LL	% Correct	HL Stat
144.9	0	1	1	0	0.010988	0.010988	0.989012	-0.01105	100	0.01111
149	0	1	1	0	0.016281	0.016281	0.983719	-0.01641	100	0.01655
152.56	0	1	1	0	0.022859	0.022859	0.977141	-0.02312	100	0.023393
155.2	0	1	1	0	0.02935	0.02935	0.97065	-0.02979	100	0.030237
158	0	1	1	0	0.038181	0.038181	0.961819	-0.03893	100	0.039696
162.25	0	1	1	0	0.056606	0.056606	0.943394	-0.05827	100	0.060003
168	0	1	1	0	0.094968	0.094968	0.905032	-0.09978	100	0.104933
171.3	0	1	1	0	0.126347	0.126347	0.873653	-0.13507	100	0.144619
174.8	0	1	1	0	0.168902	0.168902	0.831098	-0.18501	100	0.203228
180.37	0	1	1	0	0.258844	0.258844	0.741156	-0.29954	100	0.349243
181.2	1	0	1	1	0.27462	0.27462	0.72538	-1.29237	0	2.64139
184.3	1	0	1	1	0.338505	0.338505	0.661495	-1.08322	0	1.95417
191	1	0	1	1	0.49533	0.49533	0.50467	-0.70253	0	1.018857
198.13	0	1	1	0	0.662488	0.662488	0.337512	-1.08615	0	1.962856
200.63	0	1	1	0	0.714515	0.714515	0.285485	-1.25357	0	2.502817
209.2	1	0	1	1	0.852013	0.852013	0.147987	-0.16015	100	0.173691
212.2	1	0	1	1	0.885147	0.885147	0.114853	-0.122	100	0.129756
226.3	1	0	1	1	0.968099	0.968099	0.031901	-0.03242	100	0.032952
239	1	0	1	1	0.990503	0.990503	0.009497	-0.00954	100	0.009588
248.4	1	0	1	1	0.99617	0.99617	0.00383	-0.00384	100	0.003845
270.3	1	0	1	1	0.999543	0.999543	0.000457	-0.00046	100	0.000457
278.73	1	0	1	1	0.999798	0.999798	0.000202	-0.0002	100	0.000202
308.26	1	0	1	1	0.999989	0.999989	1.14E-05	-1.1E-05	100	1.14E-05
	11	12	23			11.00004	11.99996	-6.64345	78.26087	11.41361

Figure 54 shows the predicted values with number of success, failure, and accuracy of each dataset

Classification Table			
	Suc-Obs	Fail-Obs	
Suc-Pred	10	2	12
Fail-Pred	2	9	11
	12	11	23
Accuracy	0.833333	0.818182	0.826087
Cutoff	0.5		
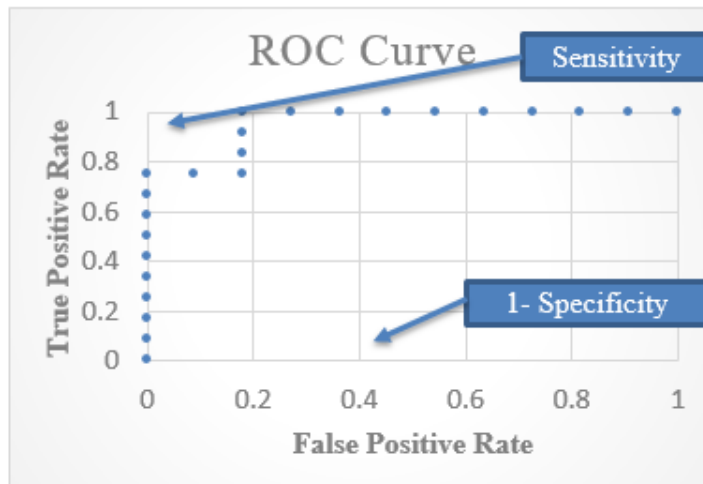
Figure 55 shows the ROC curve for logistic model.

Figure 55 shows the Receiver Operation Characteristic of the logistic regression model. The ROC is used to describe how well the logistic model did classify between full and partial weight bearing. To conclude this experiment, the peak pressure values generated from the heel contact have a good indication to identify the gait patterns between healthy and unhealthy subjects (partial foot bearing). Limited bearing is considered to play an important role for graduated recovery and strains regulation.

4.8 Preferred Transition speed

PTS is the speed that the subject would choose to alternate from walk to run mode. PTS is estimated to be 4mph. However, studies showed that when walking at a speed above the PTS, it is more likely that the metabolic energy would increase, rather than if the subject preferred to start running. Other studies illustrated that humans would select the PTS at Froude number equal to 0.5. [31].

$$Froude = \frac{v^2}{gl}$$

Where (v) stands for the locomotion velocity, (l) is the leg length, and (g) is the earth's gravity $9.81\ ms^{-2}$. MacLeod et al [32] disscued the effectivness of PTS during foot loading and unloading. A pre-set protocol assumed to load each shoe with 2 kg mass, and ask subjects to perform walking at three different speeds (60%, 80% and 100% of PTS) on a treadmill. Studies showed that the dosriflexors are important to determine the PTS level with respect to the metabolic energy. While another study showed that the "preventing overxertion of ankle dosriflexors" is what casues the alternations between walk-to-run [32]. MacLeod set four criteria to measure four variables with PTS.

1- The first goal is to estimate that the variable must change abruptly in value when the transition occurs.

2- The second is that the value of item one must return to the same level noted before.

3- The third one is to tell that the variable has provided the necessary input to signal a gait transition.

4- The fourth criterion is considered a determinant of PTS.

McLeod recruited 24 young healthy subjects to walk and run on a treadmill. However, previous research has shown that 15 minutes or less of walking on a treadmill is sufficient to have the repeatability operations [32]. Each subject asked whether the walking speed is the preferred gait indication to start collecting the data. Results of the four selected variables (ankle dorsiflexion angular velocity, angular acceleration, joint moment, and joint power) increased

statistically as the walking speed increased, and decreased when the speed returns to the lower level.

However, in this study, the author is not interested in investigating what is important to determine the PTS (Like tibialis anterior), or how it is possible that the metabolic energy would increase/decrease at different PTS level, or the overexertion of dorsiflexion – to avoid fatigued conditions. These factors are more likely important considerations to regulate the heel contact (i.e. once the foot hits the ground). The author would like to investigate at what percentage the peak pressure from the heel contact would increase if the PTS increases. The empirical results between two young healthy subjects (Av. age 20.5, av height 5.25, and av. Weight 135) showed the initial contact increased 20.5% when the PTS changed from 50% to 75% (assuming the PTS is 2 m/s). The table below shows the average of four step samples taken from the aforementioned subjects' walking.

PTS%	Av.IC. F3	STD.IC.F3	Av.IC.F2	STD.F2
50	293.3	22.97	268.15	12.03
75	353.57	18.79	323.4	16.7
100	475.1	17.04	411.4	1264

Table 9 shows the average peak pressure in KPa from 5 sample steps, and their standard deviations.
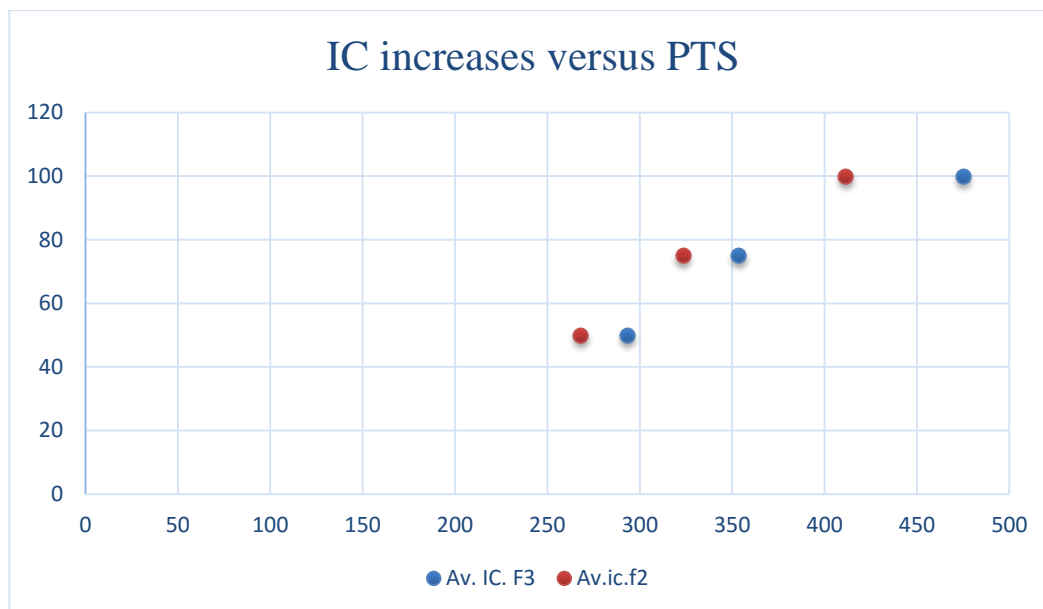
Figure 57 shows the symmetric average peak pressure (x-axis) with respect to PTS (y-axis) level at 50%, 75%, and 100%.

The motivated study allowed the researcher to collect data from 23 healthy subjects. Four out of twenty-three were dropped because of foot size and unregulated walking protocol. The nineteen remaining subjects have average weight 149, and standard deviation 19.28. Av. Age 24.1, std 4.38. Av. Height 4.38, std 0.29. Trials and protocol set to collect the data took place at Virgina Commonwealth University gym. The protocol states that each subject has to walk on a "Woodway" treadmill while they are wearing in-shoe sensors. Each subject performed walking at 50, 75, and 100% of PTS (assuming the PTS is 2 m/sec). A toggle button in Android implemented in java was set to collect the peak pressure at the local memory while the subject is on the treadmill.

The researcher has collected data every 10-15 seconds. The task was repeated at 75% and 100% of PTS as well.
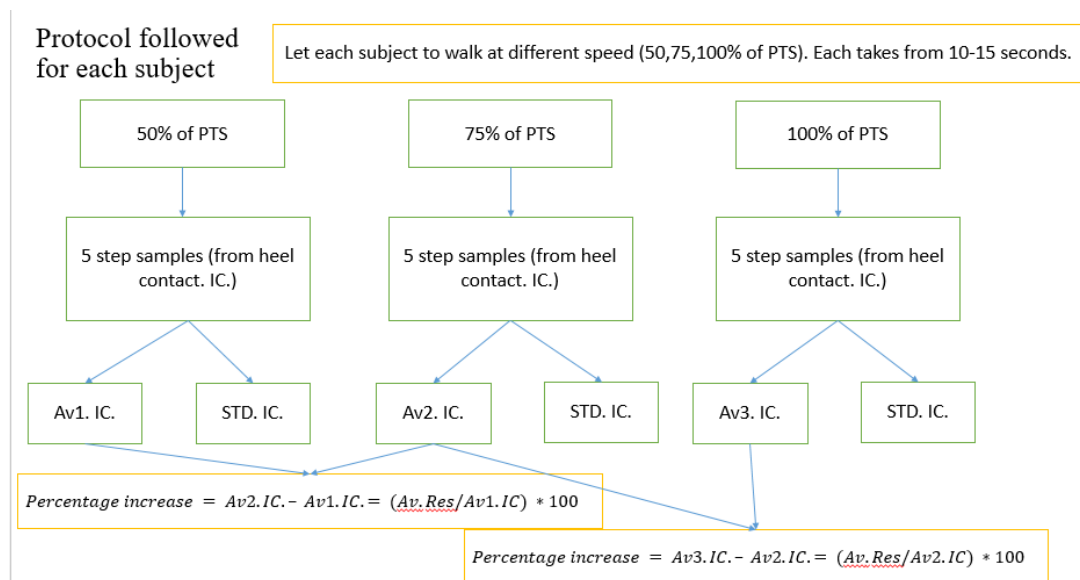
Figure 58 shows protocol followed to collect the data from each participant.

The results show that average peak pressure increased as the PTS changed from 50 to 75%. Percentage increase of initial contact (IC), ranges from 10% to 26% with average 18.32% and STD 4.78. The figure below supports the hypothesis that states that as the speed of subject increases, the peak pressure from heel contact would increase within a certain range. A symmetric scatter plot for this study is illustrated in figure 60.
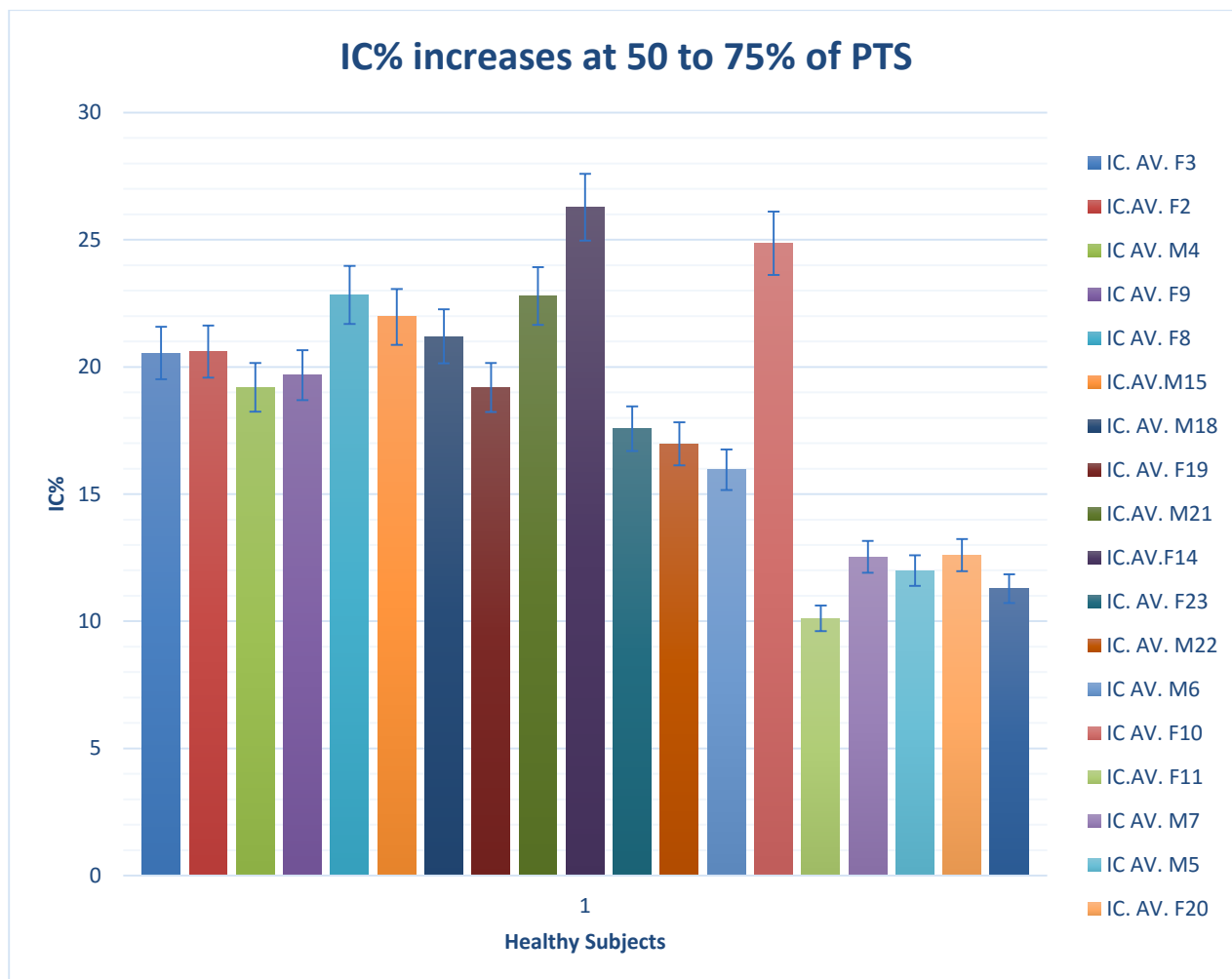
Figure 59 shows peak pressure from heel contact increases - as the speed increases
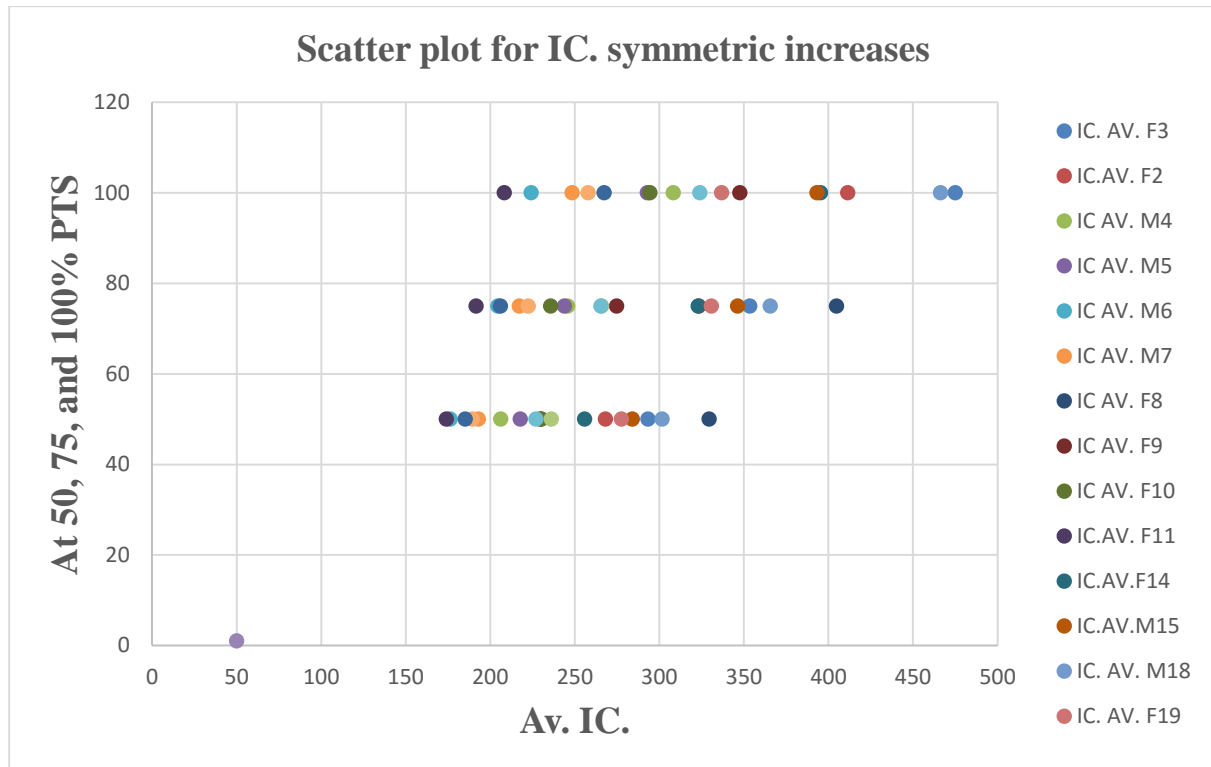
Figure 60 shows the symmetric peak pressure increases with respect the increases in speed

While 14 out of the 19 subjects showed that their peak pressure was averagely increased by 21.24% when the speed (on a treadmill) changed from 75% to 100% of the PTS, with STD 7.801. The findings of 75% to 100% increases aren't consistent, in contrast with the findings of 50 to 75%. We consider the findings useful to determine the threshold forces that affect the Achilles' tendon, as we hope these findings will be applied to relative muscle dorsiflexions to determine and reduce the level of unacceptable muscular stress when the speed changed at certain PTS [32].

IC % increase. 75 to 100% of PTS

Legend: IC. AV. F3, IC.AV. F2, IC AV. M4, IC AV. M5, IC AV. M6, IC AV. M7, IC AV. F9, IC.AV. F11, IC.AV.F14, IC.AV.M15, IC. AV. M18, IC. AV. M22, IC. AV. F23, IC. AV. M24

Figure 61 shows peak pressure percentage increased when the PTS increased from 75% to 100%

Chapter 5 Conclusion and Future work

5.1 Conclusion

The findings of this study between partial foot bearing and full load normal walk were averagely 229,2KPa and 17.9KPa respectively. The findings between two healthy subjects showed weakness linearity r=0.096, and there are no overlap between their peak pressures, but the two subjects have the same peak-to-peak time intervals. In which it concluded that the different combination of muscle can give the same results. The empirical results in GRF versus PTS showed that peak pressure has increased by 18.4% when the speed of the subject has changed from 50 to 75% of the PTS while the peak pressure has increased inconsistently by 21.2% when the speed of the subject has changed from 75 to 100% of the PTS. The investigation of alternative soluti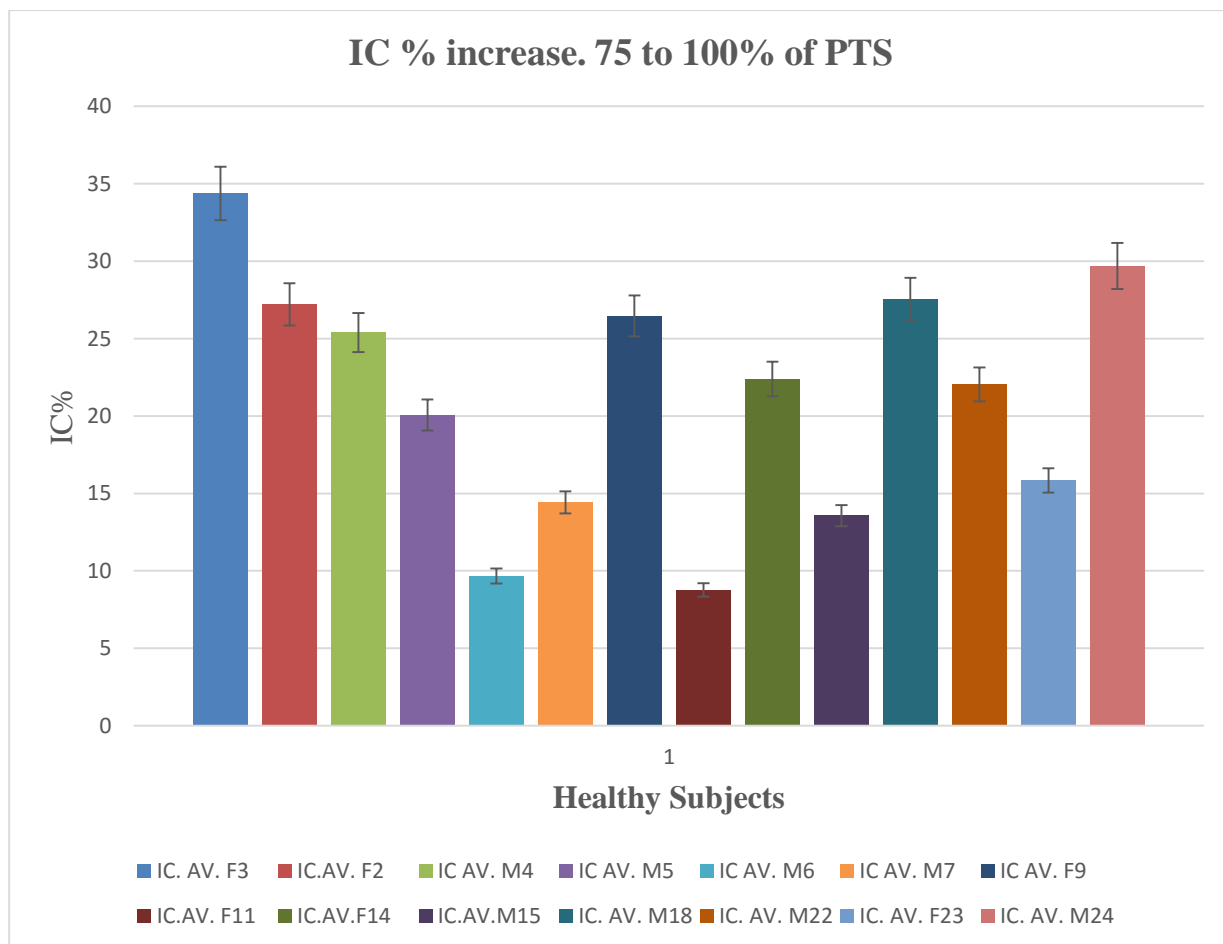ons that may supply a reliable measurement is an ongoing area of research. Over the years, researchers are in the process of competition to develop an advanced technology related to activities of daily living (ADL). The significant performance and enhancement can be achieved in sensor size, high-pressure range measurements, excellent linearity in both low and high pressures with very low hysteresis. Furthermore, the overall cost, number of sensors used, a region of interest, parameters found, and classifications are all cast for footwear and effectiveness of therapeutics. For example, in heel striking, the collision of the heel with the ground generate a significant impact transient. Regardless of the forefoot striking, the heel contact force sends the shock wave over the body using the skeletal system. Therefore, the runners avoid the large impact force that is from the heel contact. Nevertheless, the increase in the plantar foot may increase the risk of ulcers and diabetes [28].

However, the findings of this study used basic analysis of plantar pressure measurements in which it classified the pressure values from discrete foot regions (heel, 1st metatarsal, and 5th metatarsal) to the variances of walking patterns (slow - normal, normal – fast, and walking patterns between two female subjects). Gerlach Carina et al. [33] was able to identify foot ulcer based on peak pressures, relative pressure time integrals, and means of both parameters for each subject – with over six steps for each trial. Gerlach used multivariate approach and neural network classification to categorize the pressure data between healthy subjects and subjects with ulcerations. Although Gerlach used six piezoresistive sensors at the heel, midfoot, medial forefoot, middle forefoot, lateral forefoot and hallux, the in-shoe system was still not considered as suitable for outdoors. The connection used wires with a length of two meters. Therefore, it was not suitable for ADL.

 Likewise, the parameters in this study are similar to Gerlach, in which they are peak pressures from the heel, 1st metatarsal, and 5th metatarsal, peak to peak time interval and the means, which is considered as the foot stance phase and the body weight acceptance (WA).

Furthermore, the study utilized the most recent Android platform (V5.1 Lollipop – API 21) to develop a user-friendly app and to use for ADL at run time. The app is able to set threshold peak pressure with the alert set. The data acquisition used internal local memory to save the data log at any time. Where a user can recall the data to determine peak values with their time intervals as an offline system. A further development used the online monitoring system in which it can graphically demonstrate the vertical reaction force. Spatial parameters, like start-up timer, and a number of steps taken implemented to determine the cadence, speed, and stride length. The data from Android app can also send over emails as a .txt file for MATLAB

analysis. MATLAB 2011.a used the perpendicular slope and a coordinate to determine peak pressures and time intervals. The statistical approach used in MATLAB are correlation coefficient, cross correlation, hypothesis test and mean local maxima classification, in order to explicit the walking pattern between slow-normal walking, and the walking pattern between female subjects. We hope this study would direct through the investigation of possible injuries, neurological, and kinetics.

This study approved and reviewed by Institutional Review Board committee at Virginia Commonwealth University.

5.2 Future work and Discussion.

Previously discussed in logistic regression that it is a powerful tool to classify between walking pattern if and only if subjects have a unique variable can extracted from the shoe. Future work can involve online classifications between healthy and unhealthy subjects. If for example a subject's rollover patterns explicitly show a development of ulcerations, the dataset trained can classify his/her walking patterns and send over a server system to store there. On the other hand, diabetic patients could develop over time changes in foot contact phases during walking for the hope of reducing pressures in the injured area that causes overloading other plantar areas. Therefore, it may cause other severe injuries that need to be classified and taken care of [34][35].

A future work may involve a comparison between two feet (right and left), with a new prototype PCB. That kind of, run time, classification may help during injuries and hip replacements.

Bibliography

[1] Jacquelin Perry, Judith M .Gait Analysis: normal and pathological function/. Burnfield –2nd Ed. Chp 1. Thorofare, NJ 08086 USA. QP310.W3P47 2010.

[2] Abby Cain, Rachael Lowe, and Naomi O'Reilly. "Gait in prosthetic rehabilitation". Physiopedia. Network for Amputee Rehabilitation Project WCPT.UK. No 08530802. http://www.physio-pedia.com/Gait_in_prosthetic_rehabilitation

[3] Ziaei M, Nabavi SH, Mokhtarinia HR, Tabatabai Ghomshe SF. The effect of shoe sole tread groove depth on the gait parameters during walking on the dry and slippery surface. *Int J Occup Environ Med* 2013; 4:27-35.

[4] Gait Analysis: normal and pathological function/ Jacquelin Perry, Judith M. Burnfield –2nd ed. "Kinetics of Gait Ground Reaction Forces, Vectors, Moments, Power, and Pressure". Chp22. Thorofare, NJ 08086 USA. QP310.W3P47 2010.

[5] Rebecca L. Craik and Carol A. Otis. Gait Analysis: theory and application/. 1st Ed. "Foot Fall Measurement Technology" Chp. 12. Includes: Gait in humans, and Gait disorders. USA. QP310.WC73. 1994.

[6] R. M. Queen, B. B. Haynes, W. M. Hardaker, and W. E. Garrett, "Forefoot loading during 3 athletic tasks.," *Am. J. Sports Med.*, vol. 35, no. 4, pp. 630–636, 2007.

[7] L. Shu, T. Hua, Y. Wang, Q. Qiao Li, D. D. Feng, and X. Tao, "In-shoe plantar pressure measurement and analysis system based on fabric pressure sensing array.," *IEEE Trans. Inf. Technol. Biomed.*, vol. 14, no. 3, pp. 767–775, 2010.

[8] M. Saito, K. Nakajima, C. Takano, Y. Ohta, C. Sugimoto, R. Ezoe, K. Sasaki, H. Hosaka, T. Ifukube, S. Ino, and K. Yamashita, "An in-shoe device to measure plantar pressure during daily human activity," *Med. Eng. Phys.*, vol. 33, no. 5, pp. 638–645, 2011.

[9] M. Chen, B. Huang, Y. Xu, and A. Motivation, "Intelligent Shoes for Abnormal Gait Detection," pp. 2019–2024, 2008.

[10] J. J. Wertsch, J. G. Webster, and W. J. Tompkins, "A portable insole plantar pressure measurement system," *J. Rehabil. Res. Dev.*, vol. 29, no. 1, p. 13, 1992.

[11]   E. Klimiec, J. Piekarski, W. Zaraska, and B. Jasiewicz, "Electronic measurement system of foot plantar pressure", *Microelectron. Int.*, vol. 31, no. 3, pp. 229–234, 2014.

[12]. Margo N Orlin and Thomas G McPoil. "Plantar Pressure Assessment". Physical Therapy April 2000 vol. 80 no. 4 399-409.

[13]. EZ Graph. High-Rigid, Highly Precise and Wide Speed Control. SHIMADZU Excellence in Science. North America Analytical and measurement Instruments. http://www.ssi.shimadzu.com/products/product.cfm?product=ezgraph

[14]   M. Mueller, "Application of Plantar Pressure Assessment in Footwear and Insert Design," vol. 29, no. 12, pp. 747–755.

[15]   A. H. Abdul Razak, A. Zayegh, R. K. Begg, and Y. Wahab, "Foot plantar pressure measurement system: A review," *Sensors (Switzerland)*, vol. 12, no. 7, pp. 9884–9912, 2012.

[16]   I. U. Manual, "FlexiForce ® Sensors".

[17] Milette, Greg, and Stroud, Adam. Professional Android Sensor Programming (1). "Sensing the Environment". Chp 5. Somerset, US: Wrox, 2012. ProQuest ebrary. Web. 25 April 2016.

[18]. FlexiForce Starter Kit manual. "A Guide to Building Circuit for FlexiForce Sensors". Tekscan, Inc. MA. USA. www.tekscan.com/flexiforce.

[19].   Starting an Activity. Android developer's documents and Apache License. http://developer.Android.com/training/basics/activity-lifecycle/starting.html

[20].   Java. Bluetooth Class UUID. BlueCove Javadoc Apache License, Version 2.0 http://www.bluecove.org/bluecove/apidocs/javax/bluetooth/UUID.html

[21]. PhilJay / MP Android Chart. GitHub. https://github.com/PhilJay/MPAndroidChart

[22]. Truiton 2016. http://www.truiton.com/

[23].   Android Chart Example: MP Android Chart library. Truiton.com. 20 Apr, 2015 in Android tagged chart / graph by Mohit Gupt (updated on April 20, 2015). http://www.truiton.com/2015/04/Android-chart-example-mp-Android-chart-library/

[24]   C. C. Yang, Y. L. Hsu, K. S. Shih, and J. M. Lu, "Real-time gait cycle parameter recognition using a wearable accelerometry system," *Sensors*, vol. 11, no. 8, pp. 7314–7326, 2011.

[25]   M. P. De Castro, M. Meucci, D. P. Soares, P. Fonseca, M. Borgonovo-Santos, F. Sousa, L. Machado, and J. P. Vilas-Boas, "Accuracy and repeatability of the gait analysis by the walkinsense system," *Biomed Res. Int.*, vol. 2014, 2014.

[26]   R. Headon and R. Curwen, "Recognizing movements from the ground reaction force," *Proc. 2001 Work. Percetive user interfaces - PUI '01*, p. 1, 2001.

[27]   S. Pfaffen, P. Sommer, C. Stocker, R. Wattenhofer, and S. Welten, "Planipes: mobile foot pressure analysis," *Proc. First ACM Work. Mob. Syst. Appl. Serv. Healthc.*, p. 2, 2011.

[28]   S. A. Bus, R. Haspels, and T. E. Busch-Westbroek, "Evaluation and optimization of therapeutic footwear for neuropathic diabetic foot patients using in-shoe plantar pressure analysis," *Diabetes Care*, vol. 34, no. 7, pp. 1595–1600, 2011.

[29]   Hosmer, David W., Lemeshow, Stanley, and Sturdivant, Rodney X. Wiley Series in Probability and Statistics: Applied Logistic Regression (3). Chapter 3. New York, US: Wiley, 2013. ProQuest ebrary. Web. 25 April 2016.

[30]   "Logit Models for Binary Data". Chapter 3. http://data.princeton.edu/wws509/notes/c3.pdf.

[31]   Edwards, Melissa M. Scott-Pandorf, Jason R. Norcross, and Michael L. Gernhardt. The preferred walk to run transition speed in actual lunar gravity. John K. De Witt1, W. Brent. *J. Exp. Biol.*, vol. 217, pp. 3200–3203, 2014.

[32]   MacLeod, Toran D., Alan Hrelijac, and Rodney Imamura. 2014"Changes in the Preferred Transition Speed With added Mass to the Foot. Journal Of Applied Biomechanics, 30(1), 95-103.

[33]   C. Gerlach, D. Krumm, M. Illing, J. Lange, O. Kanoun, S. Odenwald, and A. Hubler, "Printed MWCNT-PDMS-Composite Pressure Sensor System for Plantar Pressure Monitoring in Ulcer Prevention," *IEEE Sens. J.*, vol. 15, no. 7, pp. 3647–3656, 2015.

[34]   I. C. N. Sacco and A. C. Amadio, "A study of biomechanical parameters in gait analysis and sensitive cronaxie of diabetic neuropathic patients," *Clin. Biomech.*, vol. 15, no. 3, pp. 196–202, 2000.

[35] D. Winter, *The biomechanics and motor control of human gait : normal, elderly, and pathological*, 2nd ed. Waterloo Ont.: University of Waterloo Press, 1991.